thereafter. CD31+ cells and CD41+ cells became detectable by day 5 and day 6, respectively, followed by the appearance of CD34+ cells. CD45+ cells became detectable after day 6, but remained low in number. c-Kit+ cells constituted about half of the cells throughout EB formation regardless of whether HOXB4 expression was induced (data not shown).
Found at: doi:10.1371/journal.pone.0004820.s006 (9.39 MB TIF)

Figure S2 Differentiation potential of individual blast colonies. Both hematopoietic and endothelial potentials were examined for individual blast colonies. Blast colonies were formed by whole EB6 cells (Fig. 3A). Colonies were individually picked up from methylcellulose and co-cultured with OP9 cells in the presence of vascular endothelial growth factor, stem cell factor, interleukin-3, TPO, and erythropoietin for 7 days. (A) The summary of hematopoietic and endothelial potentials detected in individual blast colonies. (B) Representative photomicrographs show that a colony consisted of blood cells and CD31-positive vascular endothelial cells.
Found at: doi:10.1371/journal.pone.0004820.s007 (6.61 MB TIF)

Figure S3 RT-PCR for 4 EB6 cell populations. PCR was performed on cDNAs prepared from fractionated EB6 cells.
Found at: doi:10.1371/journal.pone.0004820.s008 (3.55 MB TIF)

Figure S4 Analysis of bone marrow cells from recipient mice of HOXB4-expressing ES-derived cells. c-Kit+CD41+ EB6 cells were co-cultured with OP9 cells while HOXB4 was enforcedly expressed. After co-culture with OP9 cells, GFP+ cells and rescue cells were transplanted into lethally irradiated mice. 18 weeks after transplantation, bone marrow cells of the recipient mice were stained with antibodies and analyzed on a flow cytometer. (A–E) GFP− cells were derived from rescue cells and possibly from host cells. (F–J) GFP+ cells were derived from ESCs. GFP− cells and GFP+ cells are separately displayed for the expression of Gr-1 and Mac-1 (A, F), B220 and CD19 (B, G), CD4 and CD8 (C, H), Sca-1 and c-Kit (D, I), and CD41 and CD45 (E, J).
Found at: doi:10.1371/journal.pone.0004820.s009 (1.28 MB TIF)

Figure S5 RT-PCR analysis for induced HOXB4 expression in c-Kit+CD41+ cells. ESCs were maintained in the presence of Dox (ES HOXB4-off). After ESCs were differentiated into EB6 cells in the presence of Dox, c-Kit+CD41+ cells were isolated (c-Kit+CD41+ EB6 HOXB4-off). These cells were co-cultured with OP9 cells in the presence or absence of Dox for 4 days, followed by recovery of c-Kit+CD41+ cells from the co-cultures (c-Kit+CD41+ HOXB4-off and c-Kit+CD41+ HOXB4-on). These c-Kit+CD41+ cells and ESCs along with adult bone marrow cells (Total BM) as a negative control were examined for HOXB4 expression by RT-PCR analysis. The PCR program consisted of 15 sec at 95°C, 15 sec at 60°C, and 30 sec at 72°C. A total of 42 cycles or 30 cycles was used for amplification of HOXB4 or Gapdh.
Found at: doi:10.1371/journal.pone.0004820.s010 (9.28 MB TIF)

Figure S6 Tet-off inducible HOXB4/EGFP expression system. (A) Schematic presentation of the Tet-off HOXB4 gene expression cassette integrated into the constitutive active ROSA 26 locus on chromosome 6. HOXB4 cDNA was kindly provided by Dr. K. Humphries (Terry Fox Laboratory, Vancouver, Canada). The Tet-off regulated gene expression plasmid comprised a splice-acceptor (SA) sequence; a loxP-flanked neomycin phosphotransferase gene (neor) gene, including a polyA signal; the Tet-controlled transcriptional activator (tTA) gene, including a polyA signal; an insulator sequence; the tTA-responsive element (TRE), followed by the minimal immediate-early promoter from Cytomegalovirus (CMV); the rabbit beta-globin 2nd intron; human HOXB4 cDNA; an internal ribosome entry site (ires); EGFP cDNA; and a polyA signal. The constructed vector was amplified in E. coli Stabl2 cells (Invitrogen), purified using a GENOPURE plasmid maxi kit (Roche), linearized by SwaI digestion, and used to transfect ESCs. The Tet-regulated HOXB4/EGFP expression cassette was integrated into the constitutively active ROSA26 locus in EB3 cells by homologous recombination. In brief, EB3 ESCs were electroporated with the linearized vector and were selected with G418 (150–200 μg/ml). G418-resistant colonies were picked and ES clones carrying a targeted integration of the vector in the ROSA26 locus were identified by long distance-PCR analysis using the following primers: forward (ROSA26 locus 1st exon), 5′-CCTCGGCTAGG-TAGGGGATCGGGACTCT-3′; reverse (neor gene), 5′-CGGA-GAACCTGCGTGCAATCCATCTTGTTC-3′; forward (EGFP), 5′-GGATCACTCTCGGCATGGACGAGCTGTAC-3′; and reverse (ROSA26 locus 2nd exon), 5′-AGCCTTAAACAAG-CACTGTCCTGTCCTCAAG-3′. The PCR cycles consisted of one cycle at 94°C for 1 min, 32 cycles at 98°C for 20 s, 66°C for 30 s, 68°C for 4 min, and one cycle at 72°C for 10 min. To remove the loxP-flanked neor gene, Cre recombinase was transiently expressed in the selected clones by transfection with the pCAG-cre-IRES-puro plasmid. The resultant ES cell line was named "inducible HOXB4-EGFP ESCs" (iHOXB4 ESCs). (B) In the absence of doxycycline (Dox), tTA binds to the TRE, resulting in activation of HOXB4/EGFP transcription. In the presence of Dox, Dox binds tTA, preventing tTA binding to the TRE. We tested if this inducible expression system works in HOXB4 ES clones. Representative results from Western blot analysis for 4 clones are shown. HOXB4 was not detected when ESCs were cultured in the presence of Dox. HOXB4 was detected when ESCs were cultured in the absence of Dox. Anti-FLAG antibody was used to detect HOXB4. EGFP expression in these ES clones was consistent with results from Western blots (data not shown).
Found at: doi:10.1371/journal.pone.0004820.s011 (1.10 MB TIF)

Acknowledgments

We are grateful to Dr. A. S. Knisely for critical review of the manuscript, Drs. K. Humphries and H. Niwa, respectively, for providing human *HOXB4* cDNA and EB3 cells, and H. Meguro for assistance in DNA microarray analysis.

Author Contributions

Conceived and designed the experiments: KM HE. Performed the experiments: KM TI TN TO. Analyzed the data: KM TI TN TO KE HA HE. Contributed reagents/materials/analysis tools: SM JiM. Wrote the paper: HN HE.

References

1. Moore MAS (2004) Ontogeny of the hematopoietic system. In: Lanza R, Gearhart J, Hogan B, Melton D, Pedersen R, et al., eds. Handbook of stem cells. Burlington: Elsevier Academic Press. pp 159–174.
2. Jaffredo T, Nottingham W, Liddiard K, Bollerot K, Pouget C, et al. (2005) From hemangioblast to hematopoietic stem cell: an endothelial connection? Exp Hematol 33: 1029–1040.
3. Kennedy M, Firpo M, Choi K, Wall C, Robertson S, et al. (1997) A common precursor for primitive erythropoiesis and definitive haematopoiesis. Nature 386: 488–493.
4. Muller AM, Medvinsky A, Strouboulis J, Grosveld F, Dzierzak E (1994) Development of hematopoietic stem cell activity in the mouse embryo. Immunity 1: 291–301.

5. Cumano A, Ferraz JC, Klaine M, Di Santo JP, Godin I (2001) Intraembryonic, but not yolk sac hematopoietic precursors, isolated before circulation, provide long-term multilineage reconstitution. Immunity 15: 477–485.
6. Yoder MC, Hiatt K, Dutt P, Mukherjee P, Bodine DM, et al. (1997) Characterization of definitive lymphohematopoietic stem cells in the day 9 murine yolk sac. Immunity 7: 335–344.
7. Lacaud G, Robertson S, Palis J, Kennedy M, Keller G (2001) Regulation of hemangioblast development. Ann N Y Acad Sci 938: 96–107; discussion 108.
8. Keller G, Kennedy M, Papayannopoulou T, Wiles MV (1993) Hematopoietic commitment during embryonic stem cell differentiation in culture. Mol Cell Biol 13: 473–486.
9. Choi K, Kennedy M, Kazarov A, Papadimitriou JC, Keller G (1998) A common precursor for hematopoietic and endothelial cells. Development 125: 725–732.
10. Nishikawa SI, Nishikawa S, Hirashima M, Matsuyoshi N, Kodama H (1998) Progressive lineage analysis by cell sorting and culture identifies FLK1+VE-cadherin+ cells at a diverging point of endothelial and hemopoietic lineages. Development 125: 1747–1757.
11. Kyba M, Perlingeiro RC, Daley GQ (2002) HoxB4 confers definitive lymphoid-myeloid engraftment potential on embryonic stem cell and yolk sac hematopoietic progenitors. Cell 109: 29–37.
12. Wang N, Satoskar A, Faubion W, Howie D, Okamoto S, et al. (2004) The cell surface receptor SLAM controls T cell and macrophage functions. J Exp Med 199: 1255–1264.
13. Lengerke C, Schmitt S, Bowman TV, Jang IH, Maouche-Chretien L, et al. (2008) BMP and Wnt specify hematopoietic fate by activation of the Cdx-Hox pathway. Cell Stem Cell 2: 72–82.
14. McKinney-Freeman SL, Lengerke C, Jang IH, Schmitt S, Wang Y, et al. (2008) Modulation of murine embryonic stem cell-derived CD41+c-kit+ hematopoietic progenitors by ectopic expression of Cdx genes. Blood 111: 4944–4953.
15. Ferkowicz MJ, Starr M, Xie X, Li W, Johnson SA, et al. (2003) CD41 expression defines the onset of primitive and definitive hematopoiesis in the murine embryo. Development 130: 4393–4403.
16. Mikkola HK, Fujiwara Y, Schlaeger TM, Traver D, Orkin SH (2003) Expression of CD41 marks the initiation of definitive hematopoiesis in the mouse embryo. Blood 101: 508–516.
17. Emambokus NR, Frampton J (2003) The glycoprotein IIb molecule is expressed on early murine hematopoietic progenitors and regulates their numbers in sites of hematopoiesis. Immunity 19: 33–45.
18. Bertrand JY, Giroux S, Golub R, Klaine M, Jalil A, et al. (2005) Characterization of purified intraembryonic hematopoietic stem cells as a tool to define their site of origin. Proc Natl Acad Sci U S A 102: 134–139.
19. Matsubara A, Iwama A, Yamazaki S, Furuta C, Hirasawa R, et al. (2005) Endomucin, a CD34-like sialomucin, marks hematopoietic stem cells throughout development. J Exp Med 202: 1483–1492.
20. Furuta C, Ema H, Takayanagi S, Ogaeri T, Okamura D, et al. (2006) Discordant developmental waves of angioblasts and hemangioblasts in the early gastrulating mouse embryo. Development 133: 2771–2779.
21. Fujimoto T, Ogawa M, Minegishi N, Yoshida H, Yokomizo T, et al. (2001) Step-wise divergence of primitive and definitive haematopoietic and endothelial cell lineages during embryonic stem cell differentiation. Genes Cells 6: 1113–1127.
22. Ito T, Tajima F, Ogawa M (2000) Developmental changes of CD34 expression by murine hematopoietic stem cells. Exp Hematol 28: 1269–1273.
23. Matsuoka S, Ebihara Y, Xu M, Ishii T, Sugiyama D, et al. (2001) CD34 expression on long-term repopulating hematopoietic stem cells changes during developmental stages. Blood 97: 419–425.
24. Sauvageau G, Thorsteinsdottir U, Eaves CJ, Lawrence HJ, Largman C, et al. (1995) Overexpression of HOXB4 in hematopoietic cells causes the selective expansion of more primitive populations in vitro and in vivo. Genes Dev 9: 1753–1765.
25. Smith RA, Glomski CA (1982) "Hemogenic endothelium" of the embryonic aorta: Does it exist? Dev Comp Immunol 6: 359–368.
26. Osawa M, Hanada K, Hamada H, Nakauchi H (1996) Long-term lymphohematopoietic reconstitution by a single CD34-low/negative hematopoietic stem cell. Science 273: 242–245.
27. Morrison SJ, Hemmati HD, Wandycz AM, Weissman IL (1995) The purification and characterization of fetal liver hematopoietic stem cells. Proc Natl Acad Sci U S A 92: 10302–10306.
28. Okada S, Nakauchi H, Nagayoshi K, Nishikawa S, Nishikawa S, et al. (1991) Enrichment and characterization of murine hematopoietic stem cells that express c-kit molecule. Blood 78: 1706–1712.
29. Keller G (2005) Embryonic stem cell differentiation: emergence of a new era in biology and medicine. Genes Dev 19: 1129–1155.
30. Nobuhisa I, Ohtsu N, Okada S, Nakagata N, Taga T (2007) Identification of a population of cells with hematopoietic stem cell properties in mouse aorta-gonad-mesonephros cultures. Exp Cell Res 313: 965–974.
31. Schiedlmeier B, Santos AC, Ribeiro A, Moncaut N, Lesinski D, et al. (2007) HOXB4's road map to stem cell expansion. Proc Natl Acad Sci U S A 104: 16952–16957.
32. Sanchez MJ, Holmes A, Miles C, Dzierzak E (1996) Characterization of the first definitive hematopoietic stem cells in the AGM and liver of the mouse embryo. Immunity 5: 513–525.
33. Kiel MJ, Yilmaz OH, Iwashita T, Yilmaz OH, Terhorst C, et al. (2005) SLAM family receptors distinguish hematopoietic stem and progenitor cells and reveal endothelial niches for stem cells. Cell 121: 1109–1121.
34. Kim I, He S, Yilmaz OH, Kiel MJ, Morrison SJ (2006) Enhanced purification of fetal liver hematopoietic stem cells using SLAM family receptors. Blood 108: 737–744.
35. Suzuki A, Andrew DP, Gonzalo JA, Fukumoto M, Spellberg J, et al. (1996) CD34-deficient mice have reduced eosinophil accumulation after allergen exposure and show a novel crossreactive 90-kD protein. Blood 87: 3550–3562.
36. Abkowitz JL, Chen J (2007) Studies of c-Mpl function distinguish the replication of hematopoietic stem cells from the expansion of differentiating clones. Blood 109: 5186–5190.
37. Takakura N, Watanabe T, Suenobu S, Yamada Y, Noda T, et al. (2000) A role for hematopoietic stem cells in promoting angiogenesis. Cell 102: 199–209.
38. Bowie MB, McKnight KD, Kent DG, McCaffrey L, Hoodless PA, et al. (2006) Hematopoietic stem cells proliferate until after birth and show a reversible phase-specific engraftment defect. J Clin Invest 116: 2808–2816.
39. Kim I, Saunders TL, Morrison SJ (2007) Sox17 dependence distinguishes the transcriptional regulation of fetal from adult hematopoietic stem cells. Cell 130: 470–483.
40. Samokhvalov IM, Samokhvalova NI, Nishikawa S (2007) Cell tracing shows the contribution of the yolk sac to adult haematopoiesis. Nature 446: 1056–1061.
41. Takahashi K, Tanabe K, Ohnuki M, Narita M, Ichisaka T, et al. (2007) Induction of pluripotent stem cells from adult human fibroblasts by defined factors. Cell 131: 861–872.
42. Yu J, Vodyanik MA, Smuga-Otto K, Antosiewicz-Bourget J, Frane JL, et al. (2007) Induced pluripotent stem cell lines derived from human somatic cells. Science 318: 1917–1920.
43. Mizoguchi H, Hayakawa T (2002) The tet-off system is more effective than the tet-on system for regulating transgene expression in a single adenovirus vector. J Gene Med 4: 240–247.
44. Miyazaki S, Miyazaki T, Tashiro F, Yamato E, Miyazaki J (2005) Development of a single-cassette system for spatiotemporal gene regulation in mice. Biochem Biophys Res Commun 338: 1083–1088.
45. Zhou S, Schuetz JD, Bunting KD, Colapietro AM, Sampath J, et al. (2001) The ABC transporter Bcrp1/ABCG2 is expressed in a wide variety of stem cells and is a molecular determinant of the side-population phenotype. Nat Med 7: 1028–1034.
46. Ema H, Takano H, Sudo K, Nakauchi H (2000) In vitro self-renewal division of hematopoietic stem cells. J Exp Med 192: 1281–1288.

Cytokine 46 (2009) 127–136

Contents lists available at ScienceDirect

Cytokine

journal homepage: www.elsevier.com/locate/issn/10434666

T cell growth control using hapten-specific antibody/interleukin-2 receptor chimera

Takahiro Sogo [a], Masahiro Kawahara [a,*], Hiroshi Ueda [a], Makoto Otsu [b], Masafumi Onodera [c], Hiromitsu Nakauchi [b], Teruyuki Nagamune [a]

[a] Department of Chemistry and Biotechnology, School of Engineering, The University of Tokyo, 7-3-1 Hongo, Bunkyo-ku, Tokyo 113-8656, Japan
[b] Division of Stem Cell Therapy, Center for Stem Cell and Regenerative Medicine, Institute of Medical Science, The University of Tokyo, 4-6-1, Shirokanedai, Minato-ku, Tokyo 108-8639, Japan
[c] Department of Genetics, National Research Institute for Child Health and Development, 2-10-1, Okura, Setagaya-ku, Tokyo 157-8535, Japan

ARTICLE INFO

Article history:
Received 9 July 2008
Received in revised form 10 December 2008
Accepted 29 December 2008

Keywords:
Chimeric receptor
Interleukin-2 receptor
Growth control
Single chain Fv
T cell

ABSTRACT

IL-2 is a cytokine that is essential for the expansion and survival of activated T cells. Although adoptive transfer of tumor-specific T cells with IL-2 is one of strategies for cancer immunotherapy, it is essential to replace IL-2 that exerts severe side effects in vivo. To solve this problem, we propose to use an antibody/IL-2R chimera, which can transduce a growth signal in response to a cognate antigen. We constructed two chimeras, in which ScFv of anti-fluorescein antibody was tethered to extracellular D2 domain of erythropoietin receptor and transmembrane/cytoplasmic domains of IL-2Rβ or γ chain. When the chimeras were co-expressed in IL-3-dependent pro-B cell line Ba/F3 and IL-2-dependent T cell line CTLL-2, gene-modified cells were selectively expanded in the absence of IL-3 and IL-2, respectively, by adding fluorescein-conjugated BSA (BSA-FL) as a cognate antigen. Growth assay revealed that the cells with the chimeras transduced a growth signal in a BSA-FL dose-dependent manner. Furthermore, STAT3, STAT5, ERK1/2 and Akt, which are hallmarks for IL-2R signaling, were all activated by the chimeras in CTLL-2 transfectant. We also demonstrated that the chimeras were functional in murine primary T cells. These results demonstrate that the antibody/IL-2R chimeras could substantially mimic the wild-type IL-2R and could specifically expand gene-modified T cells in the presence of the cognate antigen.

1. Introduction

Interleukin-2 (IL-2) is an important immunomodulatory cytokine that promotes proliferation, activation and differentiation of T cells, and is also necessary for B cell and natural killer (NK) cell function. IL-2 binds to IL-2 receptor (IL-2R) consisting of three subunits, i.e. IL-2Rα, IL-2Rβ and IL-2Rγ chains, and induces heterotrimerization of them, followed by signal transduction. IL-2Rα alone or IL-2Rβ alone has low affinity ($K_d \approx 10$ nM or ≈100 nM) to IL-2, while IL-2Rγ alone has no detectable affinity to IL-2. A high-affinity receptor ($K_d \approx 10$ pM) is composed of all three chains, whereas in the absence of IL-2Rα expression, the other two chains have intermediate affinity ($K_d \approx 1$ nM) to IL-2 [1,2]. Naïve T cells express IL-2Rγ and low levels of IL-2Rβ, but do not express IL-2Rα, resulting in less sensitivity to IL-2. The expression of IL-2Rα is restricted to activated T cells through activation of T cell antigen receptor-mediated signaling, and allows the cells to respond to IL-2 for proliferation. Although IL-2Rα is required for the high-affinity receptor complex, IL-2Rα is dispensable for signaling, since ectopic expression of either c-kit/IL-2Rβ and c-kit/IL-2Rγ chimeras or GM-CSFRα/IL-2Rγ and GM-CSFRβ/IL-2Rβ chimeras induced ligand-dependent cell proliferation of CTLL-2 T cell line [3]. These results demonstrated that a heterodimerization of IL-2Rβ and γ chains may be sufficient for transducing growth signal in T cells.

Genetic modification of T cells is an effective approach to improve anti-cancer immunotherapy and to study T cell functions. Many investigators have tried to utilize T cells for cancer immunotherapy. One promising approach is an adoptive transfer therapy, in which tumor-specific autologous T cells are isolated, expanded in vitro and reinfused with IL-2 for further expansion in vivo [4–8]. The problem is that because most tumor antigens have very low antigenicity and their expression levels are low, rapid expansion and long-lasting maintenance of a large number of tumor-specific T cells are difficult in vivo, leading to insufficient therapeutic effect. In fact, the targets of previous reports and clinical trials have been restricted to the tumors having high antigenicity like melanoma cells and viral-antigen-expressing tumors [9–11]. Therefore, expansion of transferred T cells in vivo is critical for an efficient immunotherapy. However, T cell expansion by administrating high-dose IL-2 causes undesirable side effects such as vascular leak syndrome, and cardiac and pulmonary dysfunction, because IL-2 also directly or indirectly activates several other immune cells including NK cells, B cells, neutrophils and macrophages [12,13]. One possible clue to overcome this problem is to genetically mod-

* Corresponding author. Fax: +81 3 5841 8657.
E-mail address: kawahara@bio.t.u-tokyo.ac.jp (M. Kawahara).

1043-4666/$ - see front matter © 2009 Elsevier Ltd. All rights reserved.
doi:10.1016/j.cyto.2008.12.020

ify autologous T cells with an engineered IL-2R that could respond to non-toxic substance.

We previously developed an antigen-mediated genetically modified cell amplification (AMEGA) system using an antibody/receptor chimera that triggers a growth signal in response to a specific antigen [14–16]. An anti-fluorescein single-chain Fv (ScFv) was fused to extracellular D2 domain of erythropoietin receptor (EpoR) and transmembrane and cytoplasmic domains of gp130 to create an antibody/receptor chimera (ScFvg). When IL-3-dependent murine pro-B cell line Ba/F3 was transduced with the antibody/receptor chimera, fluorescein-conjugated BSA (BSA-FL) induced oligomerization of ScFvg chains, enabling cell growth in the medium containing BSA-FL but without IL-3 [15]. In this study, we replaced the cytoplasmic domain of ScFvg with that of IL-2Rβ and γ chains to construct antibody/IL-2R chimeras that can mimic an IL-2-mediated growth signal with BSA-FL-mediated one (Fig. 1A). We investigated whether these chimeras could be functional in Ba/F3 cells, an IL-2 dependent T cell line CTLL-2 and murine primary T cells.

2. Materials and methods

2.1. Vector construction

A plasmid pBS-Eβ-IG [17] encoding a mouse IL-2Rβ chain, a plasmid pBS-I-SEγ-IG [17] encoding a mouse IL-2Rγ chain, and a retroviral vector pMK-ScFvg [18] encoding anti-FL ScFv clone 31IJ3, were used as starting constructs. pBS-Eβ-IG was digested with BspEI and NotI, and inserted into pMK-ScFvg digested with the same enzymes to make pMK-SEβ-IG. NcoI-digested pMX-ScFvgIGFP [15] was inserted into NcoI-digested pBS-ILgIGFP [19], resulting in pBS-I-Sg-IG. BspEI-NotI-digested pBS-I-LEγ-IG was subcloned into pBS-I-Sg-IG digested with the same enzymes to create pBS-I-SEγ-IG. Then pBS-I-SEγ-IG was digested with AvrII and inserted into AvrII-digested pMK-SEβ-IG, resulting in pMK-SβISγ-IG.

pGCDNsam-based retroviral expression vectors were constructed for producing retrovirus pseudotyped with a vesicular stomatitis virus G protein (VSV-G) [40,41]. pMK-SEβ-IG and pMK-SEγ-IG were digested with BspEI and BamHI and inserted into pGCDNsam-SEmpI-IG and pGCDNsam-SEmpI-IK (manuscript in preparation) digested with the same enzymes resulting in pGCDNsam-Sβ-IG and pGCDNsam-Sγ-IK, respectively. In pGCDNsam-Sβ-IG and pGCDNsam-Sγ-IK, the genes encoding chimeric Sβ chain and Sγ chain were individually inserted into upstream of IRES-EGFP and IRES-Kusabira Orange (KO) [42], respectively (Fig. 7A).

2.2. Ligand preparation

Bovine serum albumin–fluorescein isothiocyanate conjugate (BSA-FL) was purchased from Sigma (St. Louis, MO). Fluorescein dimer was prepared as described previously [15]. The sequences of

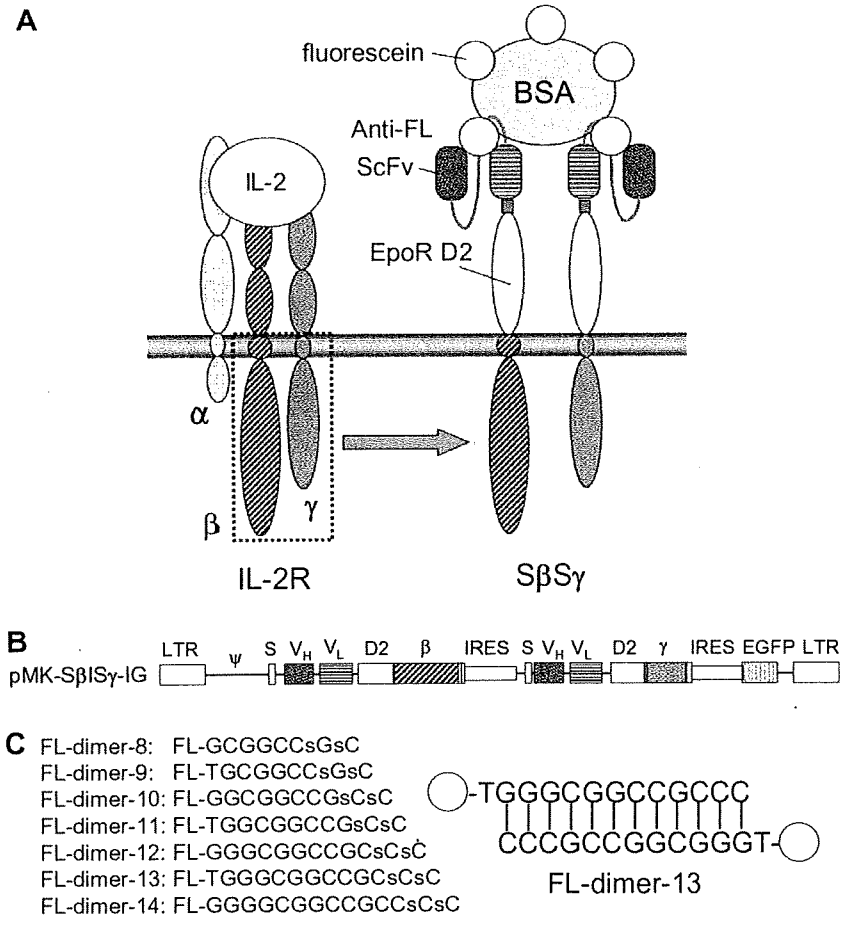

Fig. 1. The constructs of chimeric receptor and FL-dimers. (A) The schematic illustration of wild-type and chimeric IL-2R. (B) The construction of chimeric IL-2R vector. A retroviral vector with long terminal repeats (LTRs) and a packaging signal (Ψ) was used. An immunoglobulin heavy chain secretion signal sequence (S) is placed upstream of the chimeric receptor genes for cell surface expression. (C) The constructs of FL-dimers. Several lengths of fluorescein-conjugated palindromic DNAs (8–14 mer) were self-annealed to make FL-dimers. The illustration of FL-dimer-13 is shown as a representative.

the palindromic DNA linkers were as follows: 8 mer, FL-GCGG CCsGsC; 9 mer, FL-TGCGGCCsGsC; 10 mer, FL-GGCGGCCGsCsC; 11 mer, FL-TGGCGGCCGsCsC; 12 mer, FL-GGGCGGCCGCsCsC; 13 mer, FL-TGGGCGGCCGCsCsC; 14 mer, FL-GGGGCGGCCGCCsCsC. The 3′-terminal two bases in each FL-labeled DNA were made with s-oligo to prevent degradation by exonucleases. These FL-labeled s-oligo DNAs were purchased from Proligo (La Jolla, CA).

2.3. Cell culture

A murine IL-3-dependent pro-B cell line, Ba/F3 [20] was cultured in RPMI 1640 medium (Nissui Pharmaceutical, Tokyo, Japan) supplemented with 10% FBS (Biowest, Paris, France) and 1 ng/ml murine IL-3 (R&D systems, Cambridge, MA). A murine IL-2-dependent T cell line, CTLL-2 [21] was cultured in RPMI 1640 medium supplemented with 10% FBS, 2 ng/ml murine IL-2 (R&D systems), 1 mM sodium pyruvate, 50 μM monothioglycerol and 20 nM bathocuproine disulfonate (Sigma) [22]. We used three retroviral packaging cell lines. Plat-E [23] was cultured in Dulbecco's modified Eagle's medium (DMEM) (Nissui Pharmaceutical) supplemented with 10% FBS, 1 μg/ml puromycin (Sigma) and 10 μg/ml blasticidin (Kaken Pharmaceutical, Tokyo, Japan). 293GP was cultured in DMEM with 10% FBS. 293GPG was cultured in DMEM with 10% FBS, 2 μg/ml puromycin, 300 μg/ml G418 (Calbiochem, Darmstadt, Germany) and 1 μg/ml tetracycline (Sigma).

2.4. Vector transduction/transfection of Ba/F3 and CTLL-2

Ba/F3 cells were retrovirally transduced, as previously described [15]. In brief, Plat-E cells were transfected with the retroviral vector pMK-SβISγ-IG by lipofection and the culture medium was used as a viral supernatant. Ba/F3 cells were transduced with the viral supernatant in the presence of 10 μg/ml polybrene (Sigma) and 2 ng/ml IL-3 in a 24-well plate, and the transduced cells were designated as Ba/SβSγ. CTLL-2 cells were transfected with SspI-digested linear pMK-SβISγ-IG plasmid (20 μg) and pMXs-neo plasmid (1 μg) by electroporation in the presence of 100 μM spermine (Sigma). The cells (3×10^6 in 500 μl of RPMI medium) mixed with the vectors were transferred to a 4 mm-gap cuvette, and electroporation was performed at 300 V and 1000 μF using an Electroporator II (Invitrogen, Groningen, The Netherlands). Subsequently, transfected cells were inoculated into a 100 mm diameter dish and cultured in a 5% CO_2 incubator at 37 °C. Transfected cells were designated as CT/SβSγ.

2.5. Retroviral transduction of murine primary T cells

A retroviral packaging cell line, 293GP was co-transfected with pGCDNsam expression vector and pcDNA3.1-VSV-G vector encoding VSV-G envelope gene by lipofection for a transient production of VSV-G pseudotyped retroviruses. Culture medium of transfected 293GP was collected and subsequently used for transduction of 293GPG that had been engineered to express the VSV-G protein under control of a tetracycline-inducible system [40]. 293GPG cells transduced with pGCDNsam-Sβ-IG or pGCDNsam-Sγ-IK stably produced retroviruses encoding the respective genes. The culture supernatant of transduced 293GPG was collected and centrifuged at 6000g for 16 h at 4 °C, followed by resuspension of viral pellet in StemPro-34 SFM (Invitrogen) to obtain 100-fold concentrated virus.

To isolate mouse primary T cells, splenocytes were harvested from 10 weeks old male C57BL/6 mice (Japan SLC, Shizuoka, Japan) and labeled with anti-CD90.2 microbeads (Miltenyi, Auburn, CA), followed by magnetic cell sorting. Isolated CD90.2 positive T cells were subsequently inoculated into a 24-well plate (2×10^6 cells/well) in RPMI1640 medium supplemented with 10% FBS, 5 μM 2-mercaptoethanol, 10 ng/ml IL-2, and 20 μl Dynabeads mouse CD3/CD28 T cell expander (Invitrogen). The T cells cultured for 24 h were then seeded into a 24-well plate coated with retronectin (Takara, Shiga, Japan) with 15 μl each of Sβ-IG and Sγ-IK viral supernatants ($1–2 \times 10^8$ transducing units/ml for Jurkat cells), and incubated for 24 h in RPMI1640 with 2% FBS and 10 ng/ml IL-2. The cells were also co-transduced with two mock vectors encoding IG alone and IK alone as a negative control. After another 24 h culture in RPMI1640 with 10% FBS and 10 ng/ml IL-2, transduction efficiency of the cells were analyzed by flow cytometry.

2.6. Selection of the transfectants/transductants and cell proliferation assay

For selection of the Ba/SβSγ and CT/SβSγ, the cells were washed with PBS and inoculated into 24-well plates. Ba/SβSγ was selected in the medium containing either no factor, 5 μg/ml BSA-FL, or 1 ng/ml IL-3. CT/SβSγ was initially selected in the medium containing 2 ng/ml IL-2 and 800 μg/ml G418, followed by selection in the medium with 5 μg/ml BSA-FL. For cell proliferation assay, the selected cells were washed with PBS and were seeded into 24-well plates at 10^4 or 5×10^4 cells/ml with indicated concentrations of each ligand. The viable cell numbers were counted by a hemocytometer and trypan blue exclusion assay.

Murine primary T cells transduced with mock vectors (IG and IK), Sβ-IG alone, Sγ-IK alone and both Sβ-IG and Sγ-IK were sorted using MoFlo fluorescence-activated cell sorter (Dako, Glostrup, Denmark) and cultured with 10 ng/ml IL-2 for two days. The cells were washed twice with PBS containing 2% FBS to remove IL-2, and subsequently inoculated into a 48-well plate at 1.5×10^5 cells/well with no ligand, 5 μg/ml BSA-FL, or 10 ng/ml IL-2 and cultured for three days. Viable cells were determined as propidium iodide (PI)-negative cells and their numbers were counted by flow cytometric analysis using Flow-Count (Beckman Coulter, Fullerton, CA).

2.7. Western blotting

The cells (10^6 cells) were washed with PBS, lysed with 100 μl of lysis buffer (20 mM Hepes, 150 mM NaCl, 10% glycerol, 1% Triton X-100, 1.5 mM $MgCl_2$, 1 mM EGTA, 10 μg/ml aprotinin, 10 μg/ml leupeptin, pH 7.5) and incubated on ice for 10 min. After centrifugation at 16,000g for 10 min, the supernatant was mixed with Laemmli's sample buffer and boiled. The lysate was resolved by SDS-PAGE and transferred to a nitrocellulose membrane (Millipore, Bedford, MA). After the membrane was blocked with 5% skimmed milk or 1% BSA, the blot was probed with appropriate dilutions of primary and secondary antibodies, and detection was performed using Chemi-Lumi One (Nacalai tesque, Kyoto, Japan). The primary rabbit antibodies anti-human IL-2Rβ, anti-human IL-2Rγ, anti-mouse STAT3, anti-mouse STAT5 and anti-mouse ERK1/2 were from Santa Cruz Biotechnology (Santa Cruz, CA), anti-phospho-ERK1/2 was from Promega (Madison, WI), anti-phospho-STAT3, anti-phospho-STAT5, anti-Akt and anti-phospho-Akt were from Cell Signaling Technology (Danvers, MA). HRP-conjugated anti-rabbit IgG was from Biosource (Camarillo, CA).

2.8. Flow cytometric analysis

Ba/SβSγ and CT/SβSγ were washed once with PBS and resuspended with RPMI 1640, whereas primary T cell-transductants were washed twice with PBS containing 2% FBS and resuspended with PBS containing 2% FBS. Fluorescence intensities of EGFP, KO and PI were measured using a FACSCalibur flow cytometer (Becton Dickinson, Lexington, KY) at 488 nm excitation and fluorescence detection at 530 ± 15 nm, 585 ± 21 nm and >650 nm, respectively. Cell sorting

of transduced primary T cells was performed by MoFlo flow cytometer using fluorescence intensities of EGFP and KO as indicators.

2.9. Starvation and stimulation of cells

Cells were washed twice with PBS and starved in the depletion medium (RPMI 1640, 10% FBS) for 12 h. Cells (5×10^6–1×10^7) were stimulated with 2 ml medium containing various ligands at 37 °C. Ba/F3 and its transductants were stimulated with 1 ng/ml IL-3, 5 μg/ml BSA-FL or 0.5 μM FL-dimer (13 mer), and CTLL-2 and its transfectants were stimulated with 2 ng/ml IL-2, 5 μg/ml BSA-FL or 0.5 μM FL-dimer (13 mer). After 10- or 15-min incubation, the cells were added with 2 ml of 2 mM ice-cold Na_3VO_4 in PBS, pelleted and lysed with 100 μl/10^6 cells of lysis buffer to prepare lysates for Western blot analysis.

3. Results

3.1. Selective expansion of genetically modified cells by BSA-FL

We designed an antibody/IL-2R chimera (SβSγ) that can selectively transduce an IL-2-mediated growth signal in genetically modified cells (Fig. 1A and B). The SβSγ chimera can recognize a pair of fluorescein molecules as a cognate ligand. Besides Sβ and Sγ genes, EGFP gene was inserted in pMK-SβISγ-IG vector to facilitate identification of gene-modified cells. Previous reports described that heterologous expression of chimeric IL-2Rs in an IL-3-dependent murine pro-B cell line Ba/F3 and in an IL-2-dependent murine T cell line CTLL-2 was sufficient for their proliferation in response to cognate ligands [3]. Thus, we performed functional analysis of SβSγ chimera by using Ba/F3 and CTLL-2 cells.

Ba/F3 cells were retrovirally transduced with pMK-SβISγ-IG, whereas CTLL-2 cells, which were hardly transducible by retrovirus (data not shown), were transfected with the same vector by using electroporation. For selection of the transductant/transfectant, we used BSA-FL as a ligand, because multiple fluorescein molecules in BSA-FL would facilitate oligomerization of the chimera. Ba/F3 transductant was selected in the media with 5 μg/ml BSA-FL or 1 ng/ml IL-3 for 26 or 31 days, respectively, followed by flow cytometric analysis to examine EGFP-positive cell ratios. The EGFP-positive cell ratio of BSA-FL-selected cells was almost 100%, while those of IL-3-selected cells were similar to those before selection (Fig. 2A). As for CTLL-2 transfectant, although we first attempted selection directly in the media with BSA-FL, all the cells underwent apoptotic cell death. As it might be partly due to very low frequency of transfected cells (about 0.05%) before selection, CTLL-2 cells were co-transfected with G418-resistant gene as well as pMK-SβISγ-IG, followed by selection with 800 μg/ml G418 in the presence of IL-2 in order to increase the population of transfected cells. Consequently, almost all of the cells were EGFP-positive after 18-day culture with G418 (Fig. 2B). When these cells were subsequently cultured in the medium with 5 μg/ml BSA-FL in the absence of IL-2 and G418, they successfully grew in response to BSA-FL and selected cells were all EGFP-positive after 29-day culture (Fig. 2B). Resultant selected Ba/F3 and CTLL-2 cells were designated as Ba/SβSγ and CT/SβSγ, respectively.

To investigate whether cell proliferation during BSA-FL selection was induced by the expressed chimeric IL-2Rs, the amounts of expressed chimeric receptors were compared by Western blotting. BSA-FL-selected transfectants/transductants exclusively showed distinct bands of Sβ and Sγ migrated around 72 kDa and 52 kDa, respectively (Fig. 3A and B). These results indicate that only the cells expressing the SβSγ chimera can grow in response to BSA-FL, leading to successful mimicry of an IL-2 signal in Ba/F3 and CTLL-2 cells.

3.2. BSA-FL dose-dependent cell growth of the transfectants/transductants

We next performed cell proliferation assay to evaluate whether the growth of selected cells is promoted in a BSA-FL dose-dependent manner. When Ba/SβSγ and CT/SβSγ were cultured in the media containing various concentrations of BSA-FL, both cells showed BSA-FL dose-dependent cell proliferation (Fig. 4). The lower limits for BSA-FL-dependent cell growth were between 0.1 and 1 μg/ml for both Ba/SβSγ and CT/SβSγ, and BSA-FL concentration below 0.1 μg/ml did not induce any cell growth during the culture period tested. Therefore, SβSγ chimera could promote proliferation of genetically modified cells in a BSA-FL-dependent manner without any apparent background cell growth.

3.3. Cell growth control using dimerized fluorescein

Since BSA-FL contains an immunogenic carrier protein BSA and the distances between the fluorescein molecules are unclear, we previously designed a series of dimerized fluorescein (FL-dimers) tethered with a palindromic oligo-DNA linker [15]. The lengths and sequences of the oligo-DNA linkers for FL-dimers are shown in Fig. 1C. First we cultured Ba/SβSγ and CT/SβSγ cells with various lengths of FL-dimers ranging from FL-dimer-8 (27.2 Å) to FL-dimer-14 (47.6 Å). Ba/SβSγ cells were cultured with 1 μM of each FL-dimer for 3 days, while CT/SβSγ cells were cultured with 0.5 μM of each FL-dimer for 4 days, followed by counting the viable cell number. Consequently, the optimal length of FL-dimer was FL-dimer-12 or FL-dimer-13 for Ba/SβSγ cells and FL-dimer-13 for CT/SβSγ cells. Interestingly, both cells could hardly grow in the presence of FL-dimers-8, -9, -10 and -14 (Fig. 5A and B). Compared with our previous report of a gp130 chimera, the growth activity via the SβSγ chimera is highly dependent on the length of FL-dimer, whereas the optimal linker length was similar [15]. To investigate FL-dimer dose-dependency for cell growth, Ba/SβSγ and CT/SβSγ were cultured with various concentrations of FL-dimer-13. Both Ba/SβSγ and CT/SβSγ cells showed maximum cell proliferation at 0.5 μM, and there was no apparent difference between these two cell lines (Fig. 5C and D). The optimal concentration of the FL-dimer is consistent with the previous report of the gp130 chimera as well as growth-inhibitory effect observed at higher concentrations. These results suggest that the SβSγ chimera can be properly dimerized and activated by FL-dimer.

3.4. Activation of signaling molecules via chimeric IL-2R in response to fluorescein

Heterodimerization of IL-2Rβ/IL-2Rγ subunits triggers downstream signaling events that involve the phosphorylation of various cellular proteins. IL-2 signaling activates Jak/STAT, Ras/MAPK and PI3K/Akt pathways through cellular protein kinases [24,25]. Activated Jak1 and Jak3 are able to phosphorylate signal transducer and activator of transcription (STAT) 1, STAT3 and STAT5 molecules. Phosphorylation of STAT molecules induces their dimerization, resulting in their translocation to the nucleus, where they regulate gene transcriptions. IL-2 signaling also induces tyrosine phosphorylation of IL-2Rβ, resulting in the recruitment of Shc and Grb2, followed by the activation of Ras/MAPK pathway. Syk, which is an upstream regulator of PI3K/Akt pathway, is directly associated with IL-2Rβ and is also activated by IL-2 signaling, resulting in activation of Akt [26]. To examine whether the chimeric IL-2Rs could mimic IL-2 signaling or not, phosphorylation status of STAT3, STAT5, ERK1/2 and Akt was examined by Western blotting (Fig. 6).

When CT/SβSγ was stimulated with BSA-FL or FL-dimer-13, all signal transducers tested were phosphorylated like that stimulated

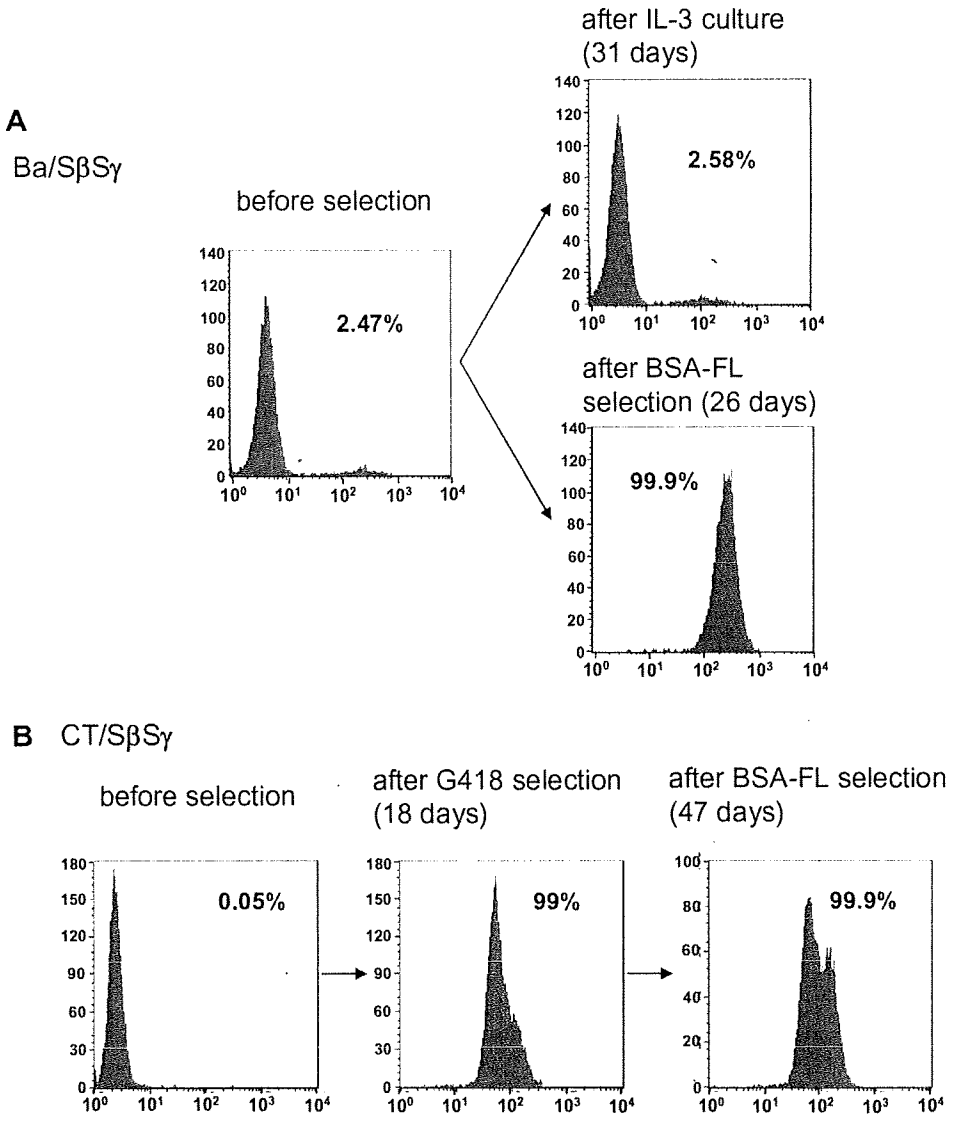

Fig. 2. Selective expansion of EGFP-positive cells with the SβSγ chimera. (A) Ba/SβSγ cells after selection with IL-3 or BSA-FL were analyzed by flow cytometry. (B) CT/SβSγ cells were selected with G418, and subsequently with BSA-FL. Cell number was plotted against log green fluorescence intensity. EGFP-negative and EGFP-positive regions were determined by taking parental Ba/F3 (A) or CTLL-2 cells (B) as a negative control. The days from gene transfer and the EGFP-positive cell ratios are indicated.

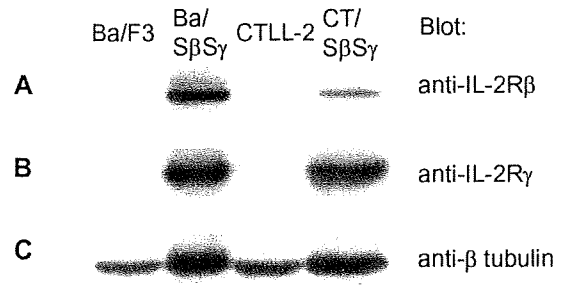

Fig. 3. Western blot analysis to confirm the expression of Sβ and Sγ chimeras in BSA-FL-selected transfectants/transductants. The expressions of chimeric IL-2Rβ (A) and IL-2Rγ (B) were detected with anti-IL-2Rβ and anti-IL-2Rγ antibodies, respectively. The expression of β-tubulin (C) was detected with anti-β tubulin antibody as a loading control.

with IL-2 (Fig. 6B), while only STAT5 and ERK1/2 were phosphorylated in BSA-FL- and FL-dimer-13-stimulated Ba/SβSγ (Fig. 6A). Based on the results of growth assay showing that Ba/SβSγ could proliferate in an antigen-dose-dependent manner (Fig. 4A and 5C), activations of STAT5 and ERK1/2 are likely to be sufficient for the growth of Ba/F3 transductant. Meanwhile, considering about the cell growth control, both Ba/SβSγ and CT/SβSγ showed strictly antigen-dose-dependent growth without any background cell growth, although STAT5 and ERK1/2 were slightly phosphorylated and Akt was constitutively activated in nonstimulated CT/SβSγ. The hyperactivations of these molecules may contribute to the subtle growth of CT/SβSγ cultured with 0.1 μg/ml BSA-FL or 0.01 μM FL-dimer-13, which was not observed in Ba/SβSγ (Fig. 4 and 5C and D). However, these hyperactivations were not strong enough for CT/SβSγ to grow without any ligand. Therefore, the SβSγ chimera can successfully control the proliferation of Ba/F3 and CTLL-2 through transducing an IL-2-like growth signal in response to the specific antigen.

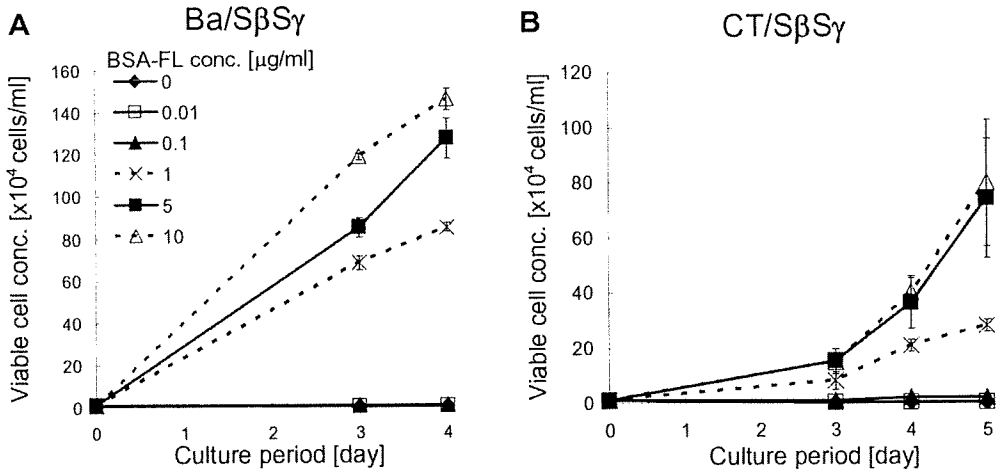

Fig. 4. BSA-FL-dependent cell growth of the transfectants/transductants. BSA-FL-selected Ba/SβSγ (A) and CT/SβSγ (B) were inoculated into 24-well plates at day 0 (10^4 cells/well) and cultured with indicated concentrations of BSA-FL. Viable cell concentration in triplicates was plotted with average and 1 SD.

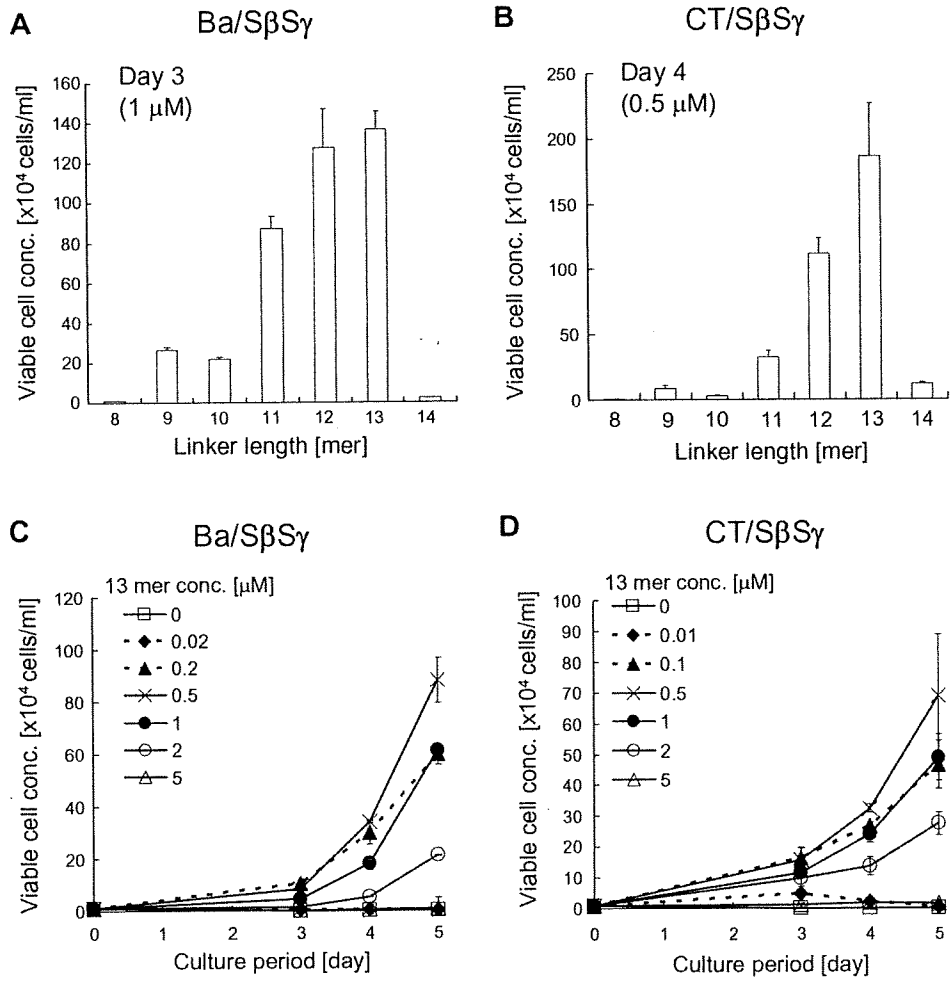

Fig. 5. FL-dimer-dependent cell growth of the transfectants/transductants. Ba/SβSγ (A) and CT/SβSγ (B) were inoculated into 24-well plates at 10^4 and 5×10^4 cells/well, respectively, and cultured with various FL-dimers. Ba/SβSγ (C) and CT/SβSγ (D) were inoculated into 24-well plates at 10^4 cells/well and cultured with indicated concentrations of FL-dimer-13. Viable cell concentration in triplicates was plotted with average and 1 SD.

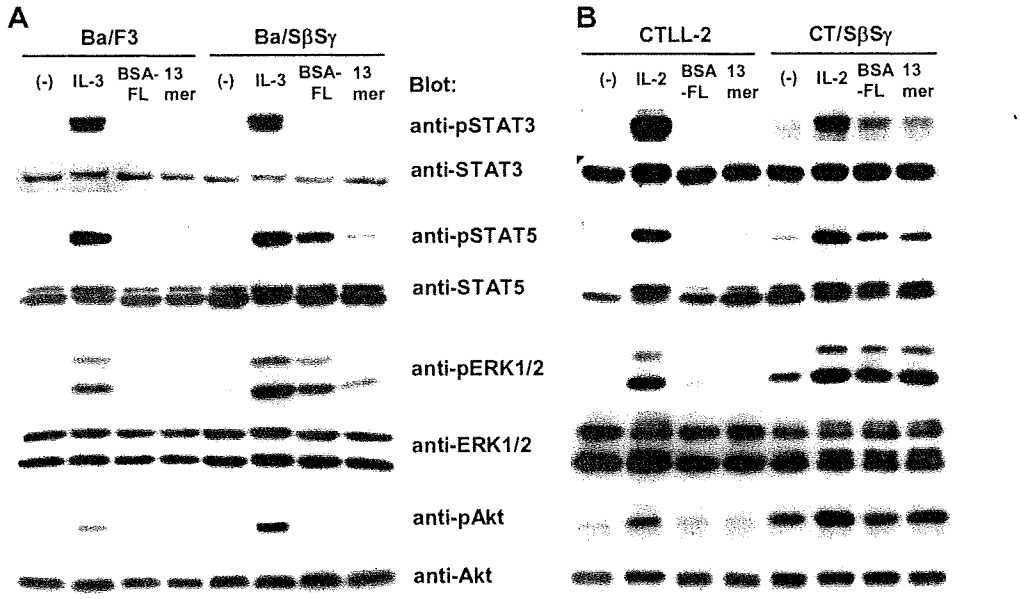

Fig. 6. Signal transduction to STAT3, STAT5, ERK1/2 and Akt. (A) Ba/F3 and Ba/SβSγ were stimulated with or without ligand (1 ng/ml IL-3, 5 μg/ml BSA-FL or 0.5 μM FL-dimer-13), and (B) CTLL-2 and CT/SβSγ were stimulated with or without ligand (2 ng/ml IL-2, 5 μg/ml BSA-FL or 0.5 μM FL-dimer-13). Western blot analysis was performed with anti-phospho STAT3, anti-phospho STAT5, anti-phospho-ERK1/2 and anti-phospho-Akt antibodies to detect phosphorylated form of each molecule, and with anti-STAT3, anti-STAT5, anti-ERK1/2 and anti-Akt antibodies to detect the whole molecules.

3.5. Chimeric IL-2R is functional in murine primary T cells

Murine primary T cells were transduced with chimeric IL-2Rs to confirm whether the chimeras are also functional in controlling a growth of primary T cells. To obtain high titers of retroviruses capable of transducing primary T cells with high efficiency, VSV-G pseudotyped retroviruses were prepared [40]. Retroviral packaging cell line, 293GPG was transduced with pGCDNsam-Sβ-IG or pGCDNsam-Sγ-IK (Fig. 7A), resulting in stable virus-producing cell lines named GPG/Sβ-IG or GPG/Sγ-IK. Sβ-IG encodes chimeric Sβ chain and EGFP genes, whereas Sγ-IK encodes chimeric Sγ chain and Kusabira Orange (KO) genes. The supernatants of GPG/Sβ-IG and GPG/Sγ-IK were 100-fold concentrated by centrifugation and used for co-transduction of murine primary T cells. The T cells expressing the chimeric Sβ chain and the chimeric Sγ chain are able to be distinguished by EGFP and KO fluorescence, respectively. Murine T cells were also co-transduced with mock vectors encoding IG and IK genes as a negative control.

Three days after transduction, EGFP and KO double positive (mock), Sβ-IG single positive (Sβ), Sγ-IK single positive (Sγ) and Sβ-IG and Sγ-IK double positive T cells (SβSγ) were sorted using fluorescence-activated cell sorter. The isolated T cells were cultured in the medium with no ligand, 5 μg/ml BSA-FL, or 10 ng/ml IL-2 for three days, followed by measuring viable cell numbers using flow cytometry (Fig. 7B). In SβSγ-transduced T cells, viable cell number was about 9-fold increased by addition of BSA-FL as compared to the cells cultured with no ligand. In Sβ-transduced T cells, viable cell number in the presence of BSA-FL was about 3-fold greater than that with no ligand. These data indicate that the SβSγ chimera is presumably functional in primary T cells, and that the Sβ chimera alone might transduce a subtle anti-apoptotic signal.

4. Discussion

In this study, we constructed an antibody/IL-2R. chimera named SβSγ, which can recognize fluorescein and transduce a growth signal independent of IL-2. Several studies using transgenic mice constitutively expressing IL-2Rα and/or IL-2Rβ, or IL-4R/IL-2Rβ chimera demonstrated that $CD8^+$ T cells from these mice showed IL-2- or IL-4-responsive proliferation [27–29]. Thus, exogenous expression of IL-2R or IL-2R chimera on T cells would be capable of inducing T cells to grow through IL-2 signaling. In our previous studies, we established an antigen-mediated genetically modified cell amplification (AMEGA) system employing an antibody/receptor chimera that triggers a growth signal in response to a cognate antigen, HEL [14] or fluorescein [15]. Based on this AMEGA concept, ScFv/IL-2Rβ plus ScFv/IL-2Rγ (SβSγ) were constructed to selectively expand genetically modified T cells, since heterodimerization of the cytoplasmic domains of IL-2Rβ and γ chains are sufficient for IL-2R signal transduction [30]. When introduced into Ba/F3 and CTLL-2 cells, the SβSγ chimera induced selective expansion of genetically modified cells in the presence of BSA-FL. Furthermore, the proliferation of Ba/F3 and CTLL-2 that were transfected with SβSγ gene was successfully controlled simply by addition of BSA-FL or FL-dimer as a cognate ligand.

According to the results from the cell proliferation assay, both Ba/SβSγ and CT/SβSγ demonstrated strictly ligand dose-dependent cell growth. Therefore, the SβSγ chimera could be useful to regulate genetically modified T cell growth in vitro and in vivo. Concerning the in vivo application of the chimera, the target cells are favorable to be expanded by a dimeric fluorescein molecule that is expected to have low immunogenicity. We used a series of dimerized fluorescein (FL-dimers) tethered with a palindromic oligo-DNA linker. To our surprise, both Ba/SβSγ and CT/SβSγ could hardly grow in the presence of FL-dimer-8, -9, -10 and -14. Interestingly, FL-dimer-13 greatly promoted the cell growth while FL-dimer-14 did not, though the lengths of their linkers are almost equal when they are annealed. As the linker of FL-dimer-13 includes a thymine residue at its 5′ end that makes it incomplete palindrome, this linker may have more flexibility than that of FL-dimer-14. Thus, the differential flexibility between FL-dimer-13

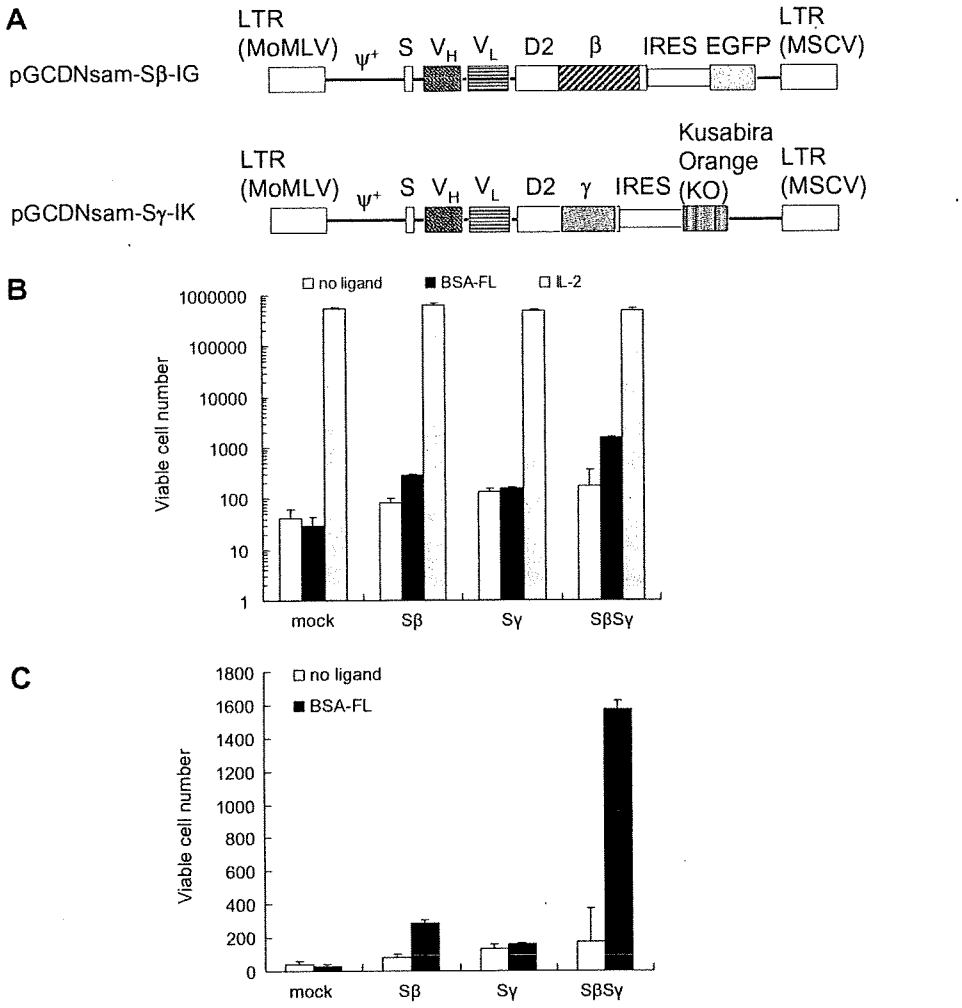

Fig. 7. Cell growth analysis of murine primary T cell-transductants. (A) The constructs of chimeric IL-2R vectors for transduction of murine primary T cells. pGCDNsam retroviral vector has 5′ MoMLV LTR, 3′ MSCV LTR and an extended packaging signal (Ψ+). (B) The mouse primary T cells were inoculated into 48-well plates at 1.5×10^5 cells/well and cultured in the medium with no ligand, 5 μg/ml BSA-FL, or 10 ng/ml IL-2 for three days. Viable cell number per well in triplicates was plotted with average and 1 SD. (C) The cells cultured with no ligand and with BSA-FL are compared using the data in (B).

and -14 might contribute to the difference of their cell growth-promoting function, while the length of FL-dimer-8, -9 and -10 might be too short to activate the SβSγ chimera. The optimal FL-dimer for the signal transduction via the SβSγ chimera was FL-dimer-12 or -13 for Ba/SβSγ and FL-dimer-13 for CT/SβSγ. These FL-dimers were similar to the optimal FL-dimer to activate a ScFv-gp130 chimera [15]. However, the growth activity via the SβSγ chimera is highly dependent on the length of FL-dimer, around 40–45 Å, in contrast to that via the ScFv-gp130 chimera, which stimulated cell growth with all lengths of FL-dimers. The optimal concentration of FL-dimer-13 for the SβSγ chimera was around 0.5 μM, which is also similar to that for ScFv-gp130 chimera. The inhibitory effect of cell growth at higher concentration of FL-dimer might be due to the preferred formation of 1:1 FL-dimer–receptor complex suppressing receptor dimerization.

Although the cell growth assay showed that both Ba/SβSγ and CT/SβSγ proliferated with similar ligand dose-dependency, immunoblot analyses indicate that the phosphorylation states of the signal transducers were greatly different between these two cell lines. STAT5 and ERK were phosphorylated in both Ba/SβSγ and CT/SβSγ when they were stimulated by BSA-FL or by FL-dimer-13, whereas STAT3 and Akt were not phosphorylated in Ba/SβSγ stimulated by the same ligands. Despite the lack of activation of STAT3 and Akt, Ba/SβSγ was able to proliferate in the presence of the ligands. These data of Ba/SβSγ are consistent with the earlier report that used Ba/F3 cells expressing randomly mutated STAT5 [31]. The report showed that the cells expressing an active form of STAT5 could grow without IL-3. Because activation of STAT5 may be sufficient for a chimeric IL-2R-mediated cell proliferation of Ba/SβSγ, the cells which were incapable of activating STAT3 and Akt could be selected by BSA-FL stimulation unlike CTLL-2 transfectant. The major difference between CTLL-2 and Ba/F3 cells is that CTLL-2 cells express wild-type IL-2Rα, whereas Ba/F3 cells do not. It has been reported that the interaction of the cytoplasmic domain of IL-2Rβ with that of IL-2Rα leads to conformational changes of IL-2Rβ [32,33]. Therefore, the existence of IL-2Rα might be a determinant for the difference of the activation state of STAT3 and Akt between Ba/SβSγ and CT/SβSγ. Nevertheless, as the SβSγ chimera successfully mimics wild-type IL-2R signaling in response to BSA-FL or FL-dimer in CT/SβSγ, we demonstrated for the first time that genetically modified T cells could be selectively expanded by a small hapten molecule.

The chimera was also functional in murine primary T cells. The SβSγ-transduced T cells showed the increased cell viability by addition of BSA-FL, indicating that the chimera has an anti-apoptotic activity in response to BSA-FL. Although BSA-FL addition increased viable cell number in SβSγ-transduced T cells, apparent cell growth was not observed. It may be because culture period was too short for the cells to grow via signals from the chimera instead of IL-2 signaling, since even cultured cell lines, Ba/SβSγ and CT/SβSγ cells, also did not proliferate in first several days of selection. To confirm this hypothesis, it is required to prolong the culture period. Interestingly, Sβ-transduced T cells also showed slight increase of viable cell number by the addition of BSA-FL. As Sβ-transduced T cells do not express Sγ chains associated with Jak3, Sβ chains might form homodimers or homooligomers to transduce Jak3-independent anti-apoptotic signals in primary T cells [3].

These data suggest that the SβSγ chimera could be utilized for the expansion of genetically modified T cells. The genetic modification of T cells is a promising approach to improve anti-cancer therapeutic effect as well as to investigate T cell function. For adoptive transfer immunotherapy using genetically modified T cells, ex vivo and in vivo T cell expansion and selection procedures are required. The selection of genetically modified T cells using cytotoxic drugs, however, causes significant cell loss and often provokes survival of undesired cells in which the transgene is not stably integrated [34]. Our system could resolve this problem, because our chimeric IL-2Rs can select genetically modified T cells by promoting their cell growth, and non-transduced cells would not survive in long-term culture without IL-2. Considering about in vivo expansion of T cells, administration of high-dose IL-2 has been the only way to expand T cells in clinical trials. However, high-dose IL-2 not only causes undesirable side effects like an inflammation, but also activates regulatory T cells that function as negative regulators of immune responses, leading to apoptosis of the effector T cells [35–37]. In this study, we succeeded in controlling cell growth in vitro using a fluorescein-specific ScFv-based chimeric IL-2R. Unlike IL-2, our system has a potential for in vivo selection without toxicity, because the SβSγ chimera enables only gene-modified T cells to proliferate in response to fluorescein derivatives, which are based on a small hapten, fluorescein, having no immunogenicity. Moreover, as there are a countless number of antigen–antibody pairs, ScFv-based chimera has the advantage that various antigens could be used for regulating cell growth as a cognate ligand. The system also has a potential for the regulation of natural immune system. It is known that NK cells, which can attack non-MHC-expressing tumor cells, are also activated by IL-2 [38,39]. Therefore, our chimeric IL-2R may be useful to control proliferation of both T cells and NK cells for an effective anti-tumor immunotherapy.

Acknowledgments

We are grateful to Dr. K. Todokoro (RIKEN) for pME-IL-2Rβ, Dr. T. Kitamura (University of Tokyo) for the retroviral expression system and Dr. I.M. Tomlinson (Domantis, Cambridge, UK) for anti-FL antibody ScFv. This work was supported by Grants-in-Aid for Scientific Research (A) 18206083 (TN) from the MEXT, Japan and the Global COE Program for Chemistry Innovation.

References

[1] Stauber DJ, Debler EW, Horton PA, Smith KA, Wilson IA. Crystal structure of the IL-2 signaling complex: paradigm for a heterotrimeric cytokine receptor. Proc Natl Acad Sci USA 2006;103:2788–93.
[2] Wang X, Rickert M, Garcia KC. Structure of the quaternary complex of interleukin-2 with its α, β, and γ_c receptors. Science 2005;310:1159–63.
[3] Nelson BH, Lord JD, Greenberg PD. Cytoplasmic domains of the interleukin-2 receptor beta and gamma chains mediate the signal for T-cell proliferation. Nature 1994;369:333–6.
[4] Leen AM, Rooney CM, Foster AE. Improving T cell therapy for cancer. Annu Rev Immunol 2007;25:243–65.
[5] Knutson KL, Almand B, Mankoff DA, Schiffman K, Disis ML. Adoptive T-cell therapy for the treatment of solid tumours. Exp Opin Biol Ther 2002;2:1–12.
[6] Rosenberg SA. Progress in human tumour immunology and immunotherapy. Nature 2001;411:380–4.
[7] Tey SK, Bollard CM, Heslop HE. Adoptive T-cell transfer in cancer immunotherapy. Immunol Cell Biol 2006;84:281–9.
[8] Cheever MA, Chen W. Therapy with cultured T cells: principles revisited. Immunol Rev 1997;157:177–94.
[9] Dudley ME, Rosenberg SA. Adoptive-cell-transfer therapy for the treatment of patients with cancer. Nat Rev Cancer 2003;3:666–75.
[10] Dudley ME, Wunderlich JR, Yang JC, Sherry RM, Topalian SL, Restifo NP, et al. Adoptive cell transfer therapy following non-myeloablative but lymphodepleting chemotherapy for the treatment of patients with refractory metastatic melanoma. J Clin Oncol 2005;23:2346–57.
[11] Koike N, Pilon-Thomas S, Mule JJ. Nonmyeloablative chemotherapy followed by T-cell adoptive transfer and dendritic cell-based vaccination results in rejection of established melanoma. J Immunother 2008;31:402–12.
[12] Kragel AH, Travis WD, Feinberg L, Pittaluga S, Striker LM, Roberts WC, et al. Pathologic findings associated with interleukin-2-based immunotherapy for cancer: a postmortem study of 19 patients. Hum Pathol 1990;21:493–502.
[13] Rosenberg SA, Lotze MT, Muul LM, Leitman S, Chang AE, Ettinghausen SE, et al. Observations on the systemic administration of autologous lymphokine-activated killer cells and recombinant interleukin-2 to patients with metastatic cancer. N Engl J Med 1985;313:1485–92.
[14] Kawahara M, Ueda H, Morita S, Tsumoto K, Kumagai I, Nagamune T. Bypassing antibiotic selection: positive screening of genetically modified cells with an antigen-dependent proliferation switch. Nucleic Acids Res 2003;31:e32.
[15] Kawahara M, Kimura H, Ueda H, Nagamune T. Selection of genetically modified cell population using hapten-specific antibody/receptor chimera. Biochem Biophys Res Commun 2004;315:132–8.
[16] Ueda H, Kawahara M, Aburatani T, Tsumoto K, Todokoro K, Suzuki E, et al. Cell-growth control by monomeric antigen: the cell surface expression of lysozyme-specific Ig V-domains fused to truncated Epo receptor. J Immunol Methods 2000;241:159–70.
[17] Sogo T, Kawahara M, Tsumoto K, Kumagai I, Ueda H, Nagamune T. Selective expansion of genetically modified T cells using an antibody/interleukin-2 receptor chimera. J Immunol Methods 2008;337:16–23.
[18] Kawahara M, Ogo Y, Ueda H, Nagamune T. Improved growth response of antibody/receptor chimera attained by the engineering of transmembrane domain. Protein Eng Des Sel 2004;17:715–9.
[19] Kaneko E, Kawahara M, Tsumoto K, Kumagai I, Ueda H, Nagamune T. Antigen-mediated genetically modified cell amplification (AMEGA) with single vector transduction. J Chem Eng Japan 2004;37:1259–64.
[20] Palacios R, Steinmetz M. IL3-dependent mouse clones that express B-220 surface antigen, contain Ig genes in germ-line configuration, and generate B lymphocyte in vivo. Cell 1985;41:727–34.
[21] Gillis S, Smith KA. Long term culture of tumour-specific cytotoxic T cells. Nature 1977;268:154–6.
[22] Brielmeier M, Bechet J, Falk MH, Pawlita M, Polack A, Bornkamm GW. Improving stable transfection efficiency: antioxidants dramatically improve the outgrowth of clones under dominant marker selection. Nucleic Acids Res 1998;26:2082–5.
[23] Morita S, Kojima T, Kitamura T. Plat-E: an efficient and stable system for transient packaging of retroviruses. Gene Ther 2000;7:1063–6.
[24] Ellery JM, Nicholls PJ. Alternate signaling pathways from the interleukin-2 receptor. Cytokine Growth Factor Rev 2002;13:27–40.
[25] Asao H. Mechanism of interleukin 2-induced signal transduction. Yamagata Med J 2003;21:141–54.
[26] Jiang K, Zhong B, Ritchey C, Gilvary DL, Hong-Geller E, Wei S, et al. Regulation of Akt-dependent cell survival by Syk and Rac. Blood 2003;101:236–44.
[27] Asano M, Ishida Y, Sabe H, Kondo M, Sugamura K, Honjo T. IL-2 can support growth of $CD8^+$ T cells but not $CD4^+$ T cells of human IL-2 receptor beta-chain transgenic mice. J Immunol 1994;153:5373–81.
[28] Gasser S, Corthesy P, Beerman F, MacDonald HR, Nabholz M. Constitutive expression of a chimeric receptor that delivers IL-2/IL-15 signals allows antigen-independent proliferation of $CD8^+$ $CD44^{high}$ but not other T cells. J Immunol 2000;164:5659–67.
[29] Nishi M, Ishida Y, Honjo T. Expression of functional interleukin-2 receptors in human light chain/Tac ransgenic mice. Nature 1988;331:267–9.
[30] Nakamura Y, Russell SM, Mess SA, Friedmann M, Erdos M, Francois C, et al. Heterodimerization of the IL-2 receptor beta- and gamma-chain cytoplasmic domains is required for signalling. Nature 1994;369:330–3.
[31] Onishi M, Nosaka T, Misawa K, Mui AL-F, Gorman D, McMahon M, et al. Identification and characterization of a constitutively active STAT5 mutant that promotes cell proliferation. Mol Cell Biol 1998;18:3871–9.
[32] Goldsmith MA, Amaral MC, Greene WC. Ligand binding by the IL-2 receptor is modulated by intracellular determinants of the IL-2 receptor β-chain. J Immunol 1995;154:2033–40.
[33] Ellery JM, Nicholls P. Possible mechanism for the alpha subunit of the interleukin-2 receptor (CD25) to influence interleukin-2 receptor signal transduction. Immunol Cell Biol 2002;80:351–7.
[34] Cooper LJN, Ausubel L, Gutierrez M, Stephan S, Shakeley R, Olivares S, et al. Manufacturing of gene-modified cytotoxic T lymphocytes for autologous cellular therapy for lymphoma. Cytotherapy 2006;8:105–17.

[35] Ahmadzadeh M, Rosenberg SA. IL-2 administration increases CD4+ CD25hi Foxp3+ regulatory T cells in cancer patients. Blood 2006;107:2409–14.
[36] Pandiyan P, Zheng L, Ishihara S, Reed J, Lenardo MJ. CD4+ CD25+ Foxp3+ regulatory T cells induce cytokine deprivation mediated apoptosis of effector CD4+ T cells. Nat Immunol 2007;8:1353–62.
[37] Wei S, Kryczek I, Edwards RP, Zou L, Szeliga W, Banerjee M, et al. Interleukin-2 administration alters the CD4+ FOXP3+ T-cell pool and tumor trafficking in patients with ovarian carcinoma. Cancer Res 2007;67:7487–94.
[38] Mule JJ, Shu S, Schwarz SL, Rosenberg SA. Adoptive immunotherapy of established pulmonary metastases with LAK cells and recombinant interleukin-2. Science 1984;225:1487–9.
[39] Bradley M, Zeytun A, Rafi-Janajreh A, Nagarkatti PS, Nagarkatti M. Role of spontaneous and interleukin-2-induced natural killer cell activity in the cytotoxicity and rejection of Fas+ and Fas− tumor cells. Blood 1998;92:4248–55.
[40] Suzuki A, Obi K, Urabe T, Hayakawa H, Yamada M, Kaneko S, Onodera M, Mizuno Y, Mochizuki H. Feasibility of ex vivo gene therapy for neurological disorders using the new retroviral vector GCDNsap packaged in the vesicular stomatitis virus G protein. J Neurochem 2002;82:953–60.
[41] Kaneko S, Nagasawa T, Nakauchi H, Onodera M. An in vivo assay for retrovirally transduced human peripheral T lymphocytes using nonobese diabetic/severe combined immunodeficiency mice. Exp Hematol 2005;33:35–41.
[42] Sanuki S, Hamanaka S, Kaneko S, Otsu M, Karasawa S, Miyawaki A, Nakauchi H, Nagasawa T, Onodera M. A new red fluorescent protein that allows efficient marking of murine hematopoietic stem cells. J Gene Med 2008;10:965–71.

Int J Hematol (2009) 89:24–33
DOI 10.1007/s12185-008-0212-2

ORIGINAL ARTICLE

Transcriptional profiling of hematopoietic stem cells by high-throughput sequencing

Yoshimi Yashiro · Hideo Bannai · Takashi Minowa · Tomohide Yabiku · Satoru Miyano · Mitsujiro Osawa · Atsushi Iwama · Hiromitsu Nakauchi

Received: 19 August 2008 / Revised: 1 October 2008 / Accepted: 23 October 2008 / Published online: 3 December 2008

Abstract Microarray analysis has made it feasible to carry out extensive gene expression profiling in a single assay. Various hematopoietic stem cell (HSC) populations have been subjected to microarray analyses and their profiles of gene expression have been reported. However, this approach is not suitable to identify novel transcripts or for profiling of genes with low expression levels. To obtain a detailed gene expression profile of $CD34^-c\text{-}Kit^+Sca\text{-}1^+$lineage marker-negative (Lin^-) ($CD34^-KSL$) HSCs, we constructed a $CD34^-KSL$ cDNA library, performed high-throughput sequencing, and compared the generated profile with that of another HSC fraction, side population (SP) Lin^- (SP Lin^-) cells. Sequencing of the 5′-termini of about 9,500 cDNAs from each HSC library identified 1,424 and 2,078 different genes from the $CD34^-KSL$ and SP Lin^- libraries, respectively. To exclude ubiquitously expressed genes including housekeeping genes, digital subtraction was successfully performed against EST databases of other organs, leaving 25 HSC-specific genes including five novel genes. Among 4,450 transcripts from the $CD34^-KSL$ cDNA library that showed no homology to the presumable protein-coding genes, 29 were identified as strong candidates for

Electronic supplementary material The online version of this article (doi:10.1007/s12185-008-0212-2) contains supplementary material, which is available to authorized users.

Y. Yashiro · M. Osawa · A. Iwama · H. Nakauchi
Division of Stem Cell Therapy,
Center for Stem Cell and Regenerative Medicine,
The Institute of Medical Science, University of Tokyo,
Tokyo 108-8639, Japan

H. Bannai · T. Yabiku · S. Miyano
Laboratory of DNA Information Analysis,
Human Genome Center, The Institute of Medical Science,
University of Tokyo, Tokyo 108-8639, Japan

Present Address:
A. Iwama
Department of Cellular and Molecular Medicine,
Graduate School of Medicine, Chiba University,
Chiba 260-8670, Japan

H. Bannai
Department of Informatics, Kyushu University,
744 Moto-oka, Nishi-ku, Fukuoka 819-0395, Japan

Present Address:
T. Yabiku
Interdisciplinary Intelligent Systems Engineering Course,
Graduate School of Engineering and Science,
Ryukyu University, Okinawa 903-0213, Japan

T. Minowa
Hitachi, Ltd, Life Science Group,
Saitama 350-1165, Japan

Present Address:
T. Minowa
Nanotechnology Innovation Center,
National Institute for Materials Science,
Ibaraki 305-0047, Japan

Present Address:
M. Osawa
Department of Developmental Biology,
University of Texas Southwestern Medical Center,
5323 Harry Hines Boulevard, Dallas, TX 75390-9133, USA

H. Nakauchi (✉)
Laboratory of Stem Cell Therapy,
Center for Experimental Medicine,
The Institute of Medical Science,
University of Tokyo, Tokyo 108-8639, Japan
e-mail: nakauchi@ims.u-tokyo.ac.jp

mRNA-like non-coding RNAs by in silico analyses. Our cyclopedic approaches may contribute to understanding of novel molecular aspects of HSC function.

Keywords Hematopoietic stem cells · High-throughput sequencing · Non-coding RNA

1 Introduction

Hematopoietic stem cells (HSCs) have the capacity to self-renew as well as the ability to differentiate into all adult hematopoietic lineages and to maintain hematopoiesis throughout the lifetime of the animal. With recent advances in cell separation systems, we now have access to highly purified HSCs. We have previously reported that in adult mouse bone marrow (BM), $CD34^{low/-}$c-$Kit^{+}Sca\text{-}1^{+}$lineage markers-negative (Lin^{-}) ($CD34^{-}KSL$) cells represent HSCs with long-term marrow repopulating ability [1]. 'Side population' (SP) cell sorting also was applied to identify HSCs [2]. SP cells are detected by their ability to efflux Hoechst 33342 dye through an adenosine triphosphate-binding cassette membrane transporter [3]. Both fractions, $CD34^{-}KSL$ and SP Lin^{-}, in mouse BM are highly enriched for long-term BM repopulating cells. The very low numbers of such repopulating cells, however, have hampered studies of HSCs, leaving the molecular nature of HSCs unknown. Recent technological innovation is overcoming this disadvantage. Microarray analyses in particular have made it feasible to carry out extensive gene expression profiling in a single assay. However, this approach is not suitable to identify novel transcripts or for profiling of genes with low expression levels. Various hematopoietic stem/progenitor cell fractions have been characterized by microarray analyses and cDNA subtraction, including mouse SP c-$Kit^{+}Sca\text{-}1^{hi}Lin^{-}$, $Thy1.1^{lo}$ c-$Kit^{+}Sca\text{-}1^{hi}Lin^{-}$, c-$Kit^{+}Sca\text{-}1^{hi}Lin^{-}Rho^{lo}$, and fetal liver c-$Kit^{+}Sca\text{-}1^{hi}Lin^{-}AA4.1^{+}$ [4–13]. Lists of HSC-specific genes are now available from several online databases such as Stem Cell Database (SCDb; http://stemcell.princeton.edu/) [12]. However, the gene expression profiles of $CD34^{-}KSL$ cells have never been directly compared with those of other HSC populations.

In this study, we constructed cDNA libraries from $CD34^{-}KSL$ and SP Lin^{-} cells by using long-distance PCR amplification of full-length cDNA, and performed high-throughput sequencing of the cDNAs yielded. Using digital subtraction against ESTs from other organ databases, we detected 25 novel genes. Furthermore, we identified 29 candidates for mRNA-like non-coding RNAs by in silico analysis. Our cyclopedic approach provides information valuable in understanding molecular aspects of HSC regulation.

2 Materials and methods

2.1 Mice

C57BL/6 (B6-Cre) mice were purchased from SLC Japan, Inc. (Hamamatsu, Japan).

2.2 Isolation of HSCs

Mouse $CD34^{-}KSL$ and SP Lin^{-} cells were purified from BM cells of 2-month-old mice. Low-density cells were isolated on Lymphoprep (1.086 g/ml; Nycomed, Oslo, Norway), and were stained with an antibody cocktail consisting of biotinylated anti-Gr-1, -Mac-1, -B220, -CD4, -CD8, and -Ter-119 mAbs (PharMingen, San Diego, CA, USA). Lineage-positive cells were depleted by passage over a MACS separation column with goat anti-rat IgG microbeads (Miltenyi Biotec, Bergisch Gladbach, Germany). The cells were further stained with fluorescein isothiocyanate (FITC)-conjugated anti-CD34, phycoerythrin (PE)-conjugated anti-Sca-1, and allophycocyanin (APC)-conjugated anti-c-Kit antibodies (PharMingen). Biotinylated antibodies were detected with streptavidin-APC-Cy7 (Molecular Probes, Eugene, OR, USA). SP Lin^{-} cells were stained with Hoechst 33342 after depleting lineage-positive cells. HSCs were isolated by fluorescence-activated cell sorting (FACS) using a MoFlo flow cytometer (DAKO Cytomation, Fort Collins, CO, USA).

2.3 Construction of HSC cDNA libraries

Total RNA was isolated from 6,000 $CD34^{-}KSL$ and 10,000 SP Lin^{-} cells using ISOGEN-LS solution (Nippon Gene, Tokyo, Japan). Total RNA was subjected to full-length cDNA synthesis using a SMART™ PCR cDNA synthesis kit (Clontech, Palo Alto, CA, USA), which is based on SMART cDNA technology and cDNA amplification by long-distance PCR. $CD34^{-}KSL$ cDNA was subcloned into the λTripEx2 phage vector (Clontech). SP Lin^{-} cDNA was subcloned into the pMX retrovirus vector [14].

2.4 Sequencing

XL1-Blue *Escherichia coli* cells were infected with the $CD34^{-}KSL$ phage library and were subcloned by plating on L Broth (LB) plates. cDNA inserts were initially amplified by standard PCR procedures on a PE 9600 thermal cycler (Applied Biosystems, Foster City, CA, USA) using the following primers: sense, 5′-CTCCGAGATCTGGACG AGC-3′, and antisense, 5′-CGTT GTAAAACGACGGC CAGTG-3′. PCR products were purified using ExoSAP-IT (Amersham Biosciences, Uppsala, Sweden) and were

sequenced using the following primer: 5′-TCTCGG GAAGCGCGCCAT-3′. The SP Lin$^-$ library was transfected by electroporation into JM109 *E. coli* cells, which then were plated on LB plates. Plasmid DNA was prepared by the alkaline-SDS method and purified by multiscreen FB filtration (Millipore, Billerica, MA, USA). Products were sequenced using the following primer: 5′-GACCTTA CACAGTCCTGCTGAC-3′.

2.5 Analysis of sequence data

A homology search of HSC library clones was performed against the RefSeq nucleotide sequence databases from the NCBI website (http://www.ncbi.nlm.nih.gov/BLAST/) using the BLASTN algorithm. Each HSC clone was assigned a Refseq identification number (ID) [15]. The clones showing the highest-scoring hits for both Identity (>95%) and Bitscore (>300.0) were selected for further analyses. Additional databases used for analyses included the Gene Ontology (GO) database from the Gene Ontology Consortium website (http://geneontology.org/) [16].

2.6 In silico subtraction

The EST databases for multiple organs, including small intestine (dbEST ID: 2601, 7229), heart (509, 5430), kidney (7215, 1300), liver (9742, 1299), and muscle (8902) were downloaded from the mouse UniGene website (http://www.ncbi.nlm.nih.gov/UniGene/). All genes were assigned a Refseq ID by BLASTN searching. Multi-organ ESTs were digitally subtracted from the HSC library clones. SCDb clones also were downloaded, assigned Refseq IDs, and compared with the HSC library clones.

2.7 Identification of putative non-coding RNAs

After homology with known protein-coding sequences according to BLASTN had been sought, remaining sequences were aligned to genomic sequence by using BLAT (http://www.genomeblat.com/genomeblat/index.asp). If they were aligned at >90% identify over >90% of their length, their cDNAs were kept; otherwise they were discarded. All of the homology searches against publicly available EST sequences were performed by BLASTN. Only EST sequences with an $E < 1.0e\text{-}100$ were regarded as corresponding to homologous mouse ESTs (ftp://ftp.ncbi.nih.gov/blast/db/est_mouse.Z). Sequences with *E*-values lower than 1.0e-50 were regarded as likely human and rat orthologous ESTs. Reverse hits were not considered.

2.8 Semi-quantitative RT-PCR

Semi-quantitative RT-PCR was carried out with normalized cDNA by quantitative PCR using TaqMan rodent GAPDH control reagent (Applied Biosystems) as described [17]. PCR products were separated on agarose gels and visualized by ethidium bromide staining.

3 Results

3.1 Cell sorting and library construction

Total RNA from 6,000 CD34$^-$KSL and 10,000 SP Lin$^-$ cells was subjected to full-length cDNA synthesis coupled with cDNA amplification by long-distance PCR. CD34$^-$KSL and SP Lin$^-$ cDNAs were, respectively, subcloned into the λTripEx2 phage vector and the pMX retrovirus vector. The sizes of the library were, respectively, 1.15×10^6 and 1.16 kb (Fig. 1). Although the two libraries were in different vectors, we used the same method for cDNA amplification and the average insert sizes were comparable with each other (CD34$^-$KSL 1.07 kb and SP Lin$^-$ 1.16 kb). Thus, we reasoned that the difference in the library construction methods did not cause any significant biases in gene expression profiles between the two populations.

3.2 Gene expression analysis

We sequenced the 5′-termini of about 9,500 cDNAs from each HSC library and compared them, using the BLASTN search algorithm, to a non-redundant database made available from the National Center for Biotechnology Information (NCBI). About 5,000 cDNAs from each library were determined to be identical to known genes in the NCBI database. These were sorted into non-overlapping sets of 1,424 and 2,077 different genes for CD34$^-$KSL and SP Lin$^-$, respectively (Fig. 2a). Most of the genes in our original collection (CD34$^-$KSL 775, SP Lin$^-$ 1,385) were represented by a single clone. In contrast, most of the genes represented by multiple cDNAs were housekeeping genes, including ubiquitin B (CD34$^-$KSL 43, SP Lin$^-$ 46), β-actin (CD34$^-$KSL 33, SP Lin$^-$ 36), ribosomal protein, and so on (Fig. 2b).

After assigning gene identities, we used reported GO to assign predictable functions to 1,034 of the CD34$^-$KSL cDNAs and 1,510 of the SP Lin$^-$ cDNAs in our set. We categorized genes by their products' subcellular localizations, biological processes, and molecular functions (Fig. 3).

We then compared gene profiles between the two HSC libraries and also with SCDb-listed HSC-specific genes

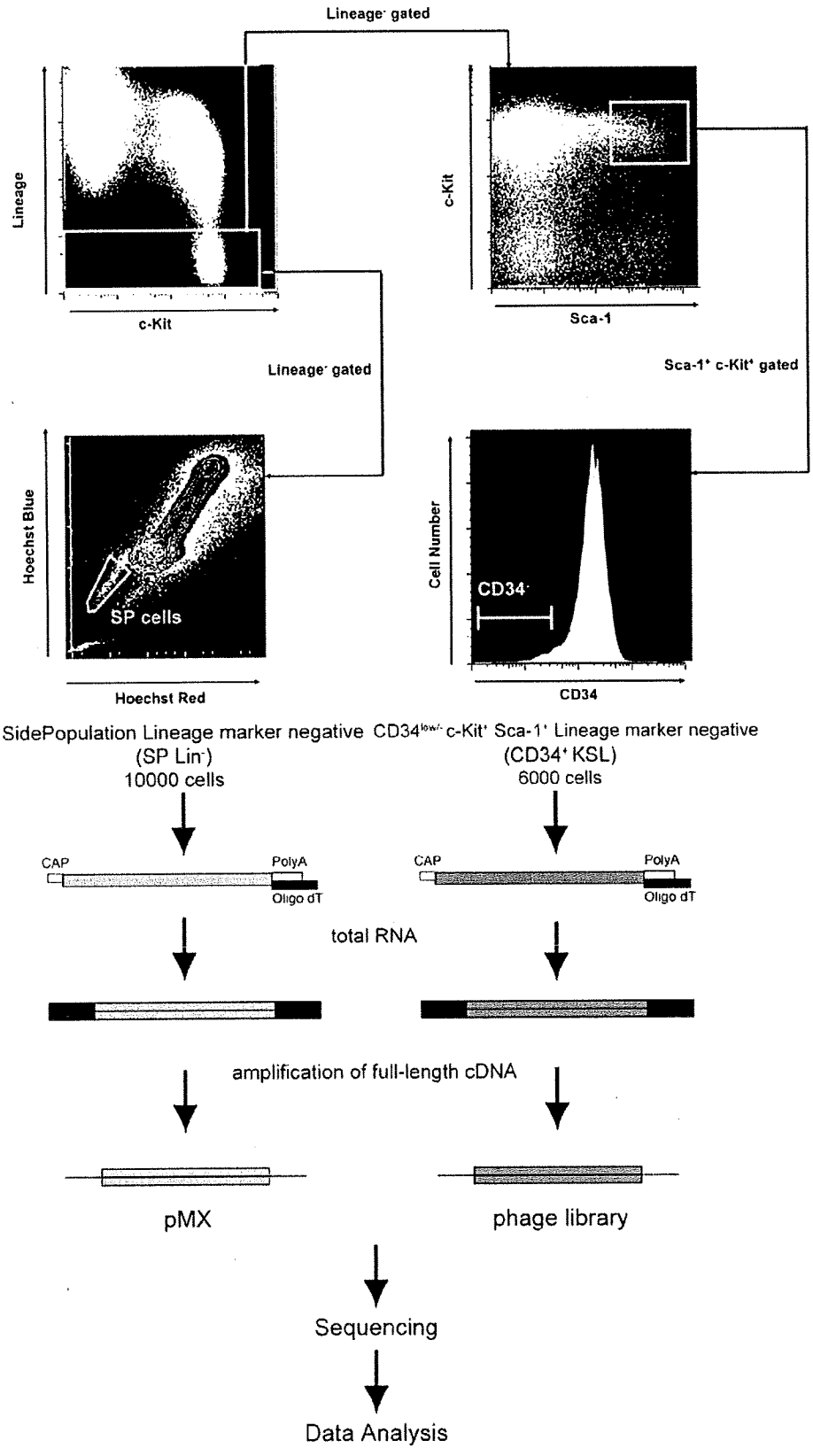

Fig. 1 Construction of the HSC cDNA libraries. Cell sorting gates for the two HSC fractions are depicted. Total RNA isolated from 6,000 CD34$^-$KSL and 10,000 SP Lin$^-$ cells was subjected to full-length cDNA *synthesis* and to cDNA amplification by long-distance PCR. CD34$^-$KSL and SP Lin$^-$ cDNAs were subcloned, respectively, into the λTripEx2 phage vector and the pMX retrovirus vector

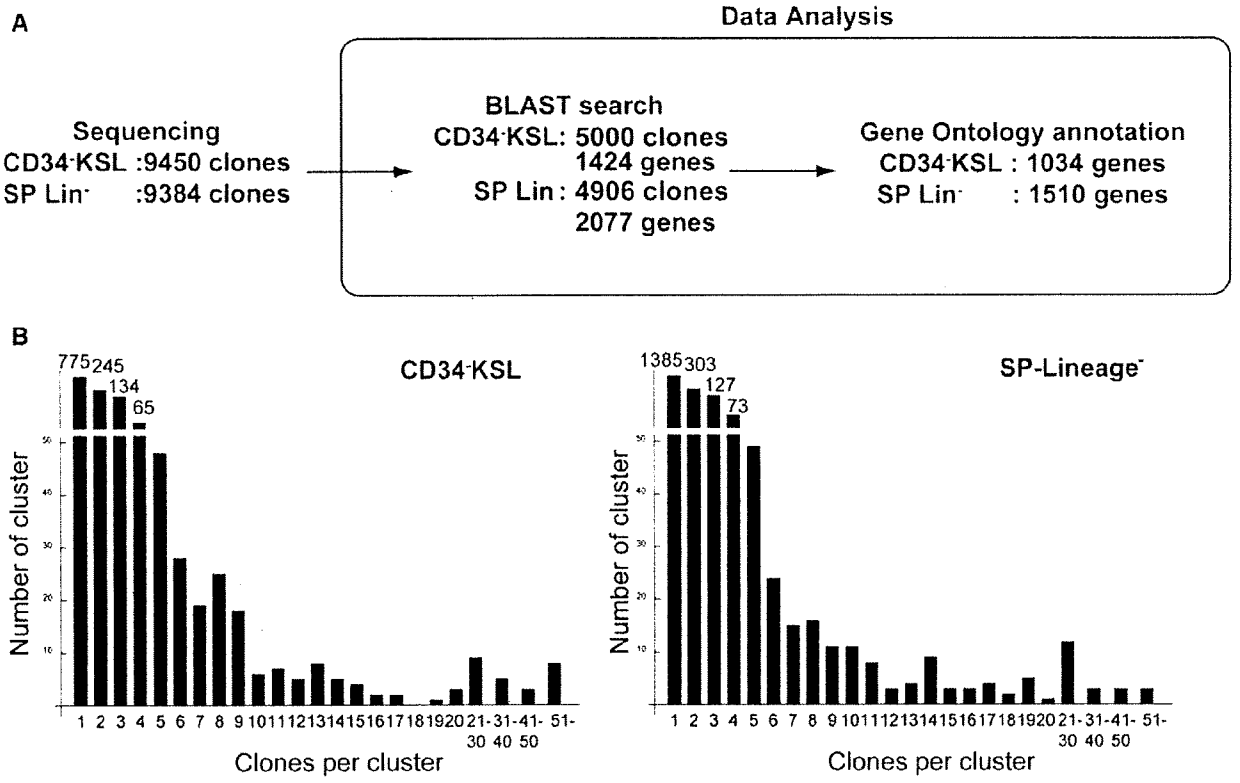

Fig. 2 Profiling of gene expression of hematopoietic stem cells by high-throughput sequencing. **a** Summary of the HSC clones identified by high-throughput sequencing. **b** Non-overlapping ESTs from CD34$^-$KSL and SP Lin$^-$ cells were assembled into clusters of singletons and contigs. The number of clusters (*Y*-axis) is plotted versus the number of clones in each cluster (*X*-axis)

[12] by using UniGene numbers to determine overlaps (Fig. 4a). To exclude ubiquitously expressed genes including housekeeping genes, digital subtraction was performed against ESTs from heart, muscle, liver, kidney, and intestine EST databases. After subtraction, 31 genes were determined to be in common between the two HSC libraries. Six of them were also included in the SCDb database (Fig. 4b). A detailed list of these genes is presented in Tables 1 and 2. Among 31 genes shared between the two HSC libraries, 25 genes appeared HSC-specific, a feature not previously reported. Of note was that five of them were novel (Fig. 4b). We next used RT-PCR to analyze these genes' expression profiles in CD34$^-$KSL and SP Lin$^-$ HSC populations. As shown in Fig. 5, we confirmed that several genes are specific to CD34$^-$KSL or to SP Lin$^-$. Others were expressed in both populations, although some genes that were not included in the SCDb database showed no HSC specificity (Table 3).

3.3 Identification of mRNA-like putative non-coding RNAs

Four thousand and four hundred and fifty clones from the CD34$^-$KSL cDNA library did not show any homology to the known protein-encoding genes in the NCBI database. We therefore computationally screened them to see if their products might include putative non-coding RNAs, the biological significance of which has recently been recognized [18, 19] (Fig. 6a).

Of these, 211 bore candidate sequences that matched the three-step criteria described in Methods (above). Among these 211, 112 clones (82 independent sequences) showed homology with known UniGene mouse ESTs. Of these 82, 55 sequences were hypothesized to represent protein-coding RNA, leaving 43 clones (29 independent sequences) as candidates for non-coding RNAs (Fig. 6b).

4 Discussion

With advances in technologies for HSC purification, many HSC populations have been subjected to gene expression profiling analyses. SCDb, one of the representative HSC databases, lists HSC-specific genes screened by high-throughput sequencing and microarray analysis of fetal liver AA4.1$^+$KSL cells and by microarray analysis of BM Rhodamine-123^{low}KSL cells. A list of HSC-specific genes has also been provided by detailed microarray analyses of

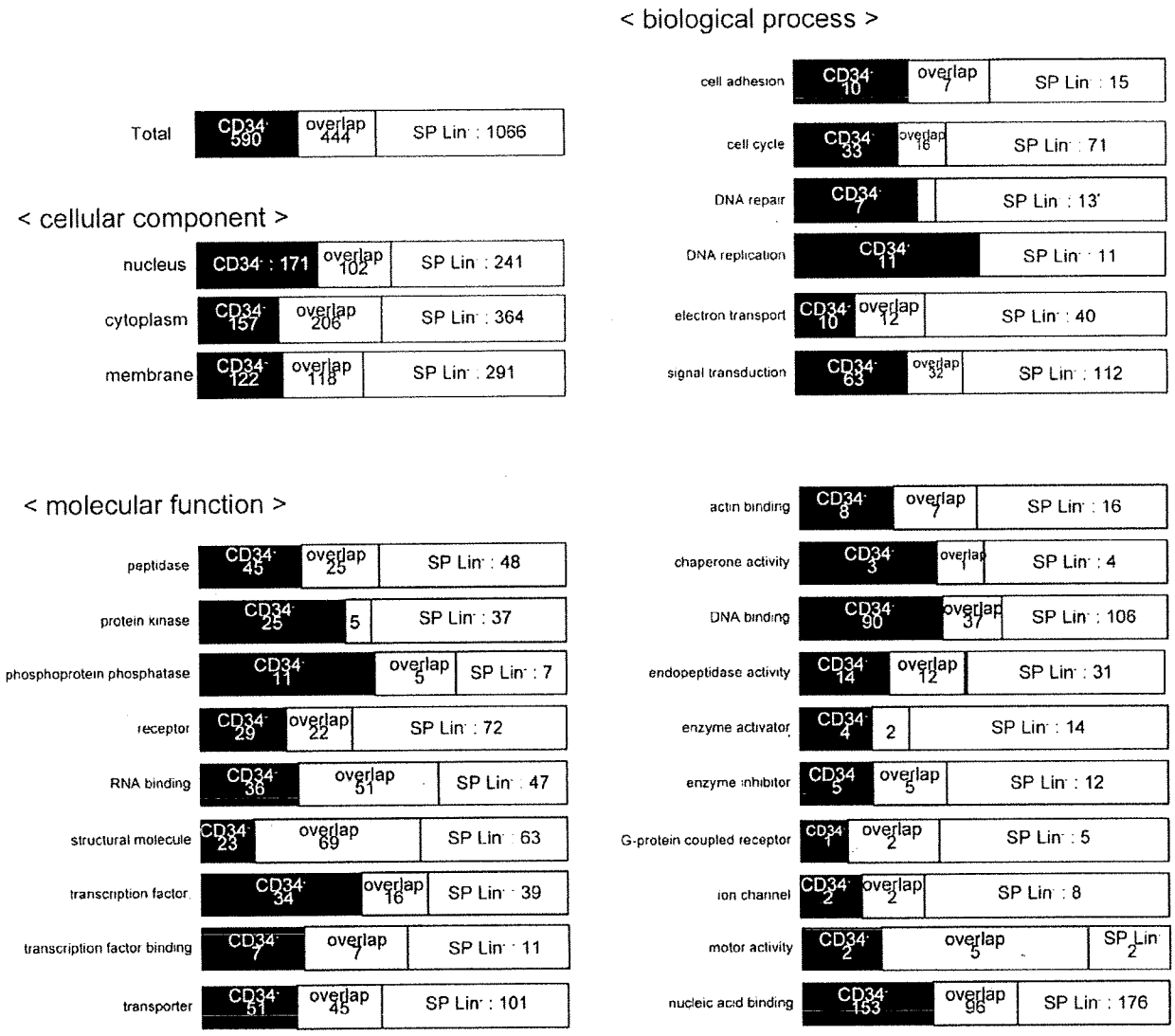

Fig. 3 Distribution of known or putative locus and functions of gene products for CD34$^-$KSL and SP Lin$^-$ genes determined by gene ontology. **a** Total, **b** cellular component, **c** molecular function, and **d** biological process

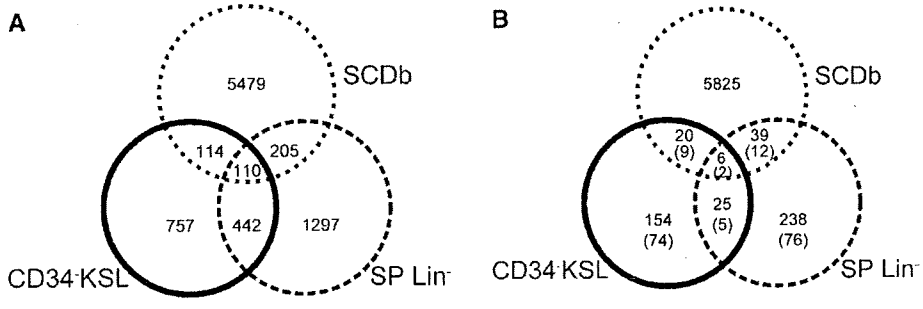

Fig. 4 Overlapping gene expression in HSCs. **a** Venn diagram detailing shared and distinct genes listed in SCDb or expressed by CD34$^-$KSL cells or by SP Lin$^-$ cells. **b** Venn diagram detailing shared and distinct genes expressed among CD34$^-$KSL cells, SP Lin$^-$ cells, and SCDb after in silico subtraction. The genes in EST databases for brain, heart, muscle, liver, kidney, and intestine were subtracted in silico from the HSC cDNAs

Table 1 Lists of genes identified as expressed in common among SCDb, $CD34^-KSL$, and SP Lin^- libraries

Accession no.	Gene
NM 008114	Growth factor independent 1B
NM 028460	RIKEN cDNA 3110045G13 gene (3110045G13Rik)
NM 008595	Manic fringe homolog (Drosophila) (Mfng)
NM 022881	Regulator of G-protein signaling 18 (Rgs18)
NM 144886	Exosome component 2 (Exosc2)
XM 354694	Serine (or cysteine) proteinase inhibitor, clade A, member 3G (Serpina3g)

$CD34^-KSL$ cells in comparison with progenitor cells and differentiated cells [20]. Furthermore, gene expression profiles have been compared among different stem cells (SP $CD34^-KSL$ HSCs, neural stem cells, and ES cells), with identification of genes expressed in common [21]. Both SP $CD34^-KSL$ and $CD34^-KSL$ cells are highly enriched for HSCs compared with fetal liver $AA4.1^+KSL$ cells. However, the paucity of SP $CD34^-KSL$ and $CD34^-KSL$ cells in BM hampered approaches to expression profiling other than microarray analysis. Cyclopedic full-length cDNA sequencing projects, however, have provided us with an abundance of cDNA data for many kinds of organs, tissues, and cells, HSCs excepted [22]. To obtain a detailed gene expression profile of $CD34^-KSL$ HSCs, we constructed a $CD34^-KSL$ cDNA library and performed high-throughput sequencing. We then compared the resultant profile with that similarly obtained for another HSC fraction, SP Lin^- cells.

The HSC libraries we constructed contained independent clones in numbers comparable with those in libraries made using similar methods (Figs. 1, 2) [23]. Successful subtraction of housekeeping genes in silico allowed us to focus on genes specific to hematopoietic cells (Fig. 4). As expected, most of the genes identified as in common among SCDb, $CD34^-KSL$, and SP Lin^- libraries appeared to be HSC-specific by RT-PCR analysis, while the genes identified as in common only between $CD34^-KSL$ and SP Lin^- libraries contained those non-specific to HSCs (Fig. 5, Table 3). Contamination with genes that are not HSC-specific also indicated the limitations of our in silico subtraction approach (Table 3). Furthermore, representative HSC genes, including *GATA-2* and *Bmi1*, were identified in only one HSC library. This might be because too few clones were sequenced. However, this approach is suitable to identify novel transcripts or for profiling of genes with low expression levels, and indeed we could identify five novel genes that are HSC-specific in expression.

By GO assignment, we predicted functions of the identified genes (Fig. 3). Among genes assessed as

Table 2 Lists of genes identified as shared only between $CD34^-KSL$ and SP Lin^- libraries

Accession no.	Gene
NM 008187	Gene trap locus 3 (Gtl3)
NM 026042	RIKEN cDNA 2810405O22 gene (2810405O22Rik)
NM 026753	RIKEN cDNA 1110019N10 gene (1110019N10Rik)
XM 127929	RIKEN cDNA 4933421G18 gene (4933421G18Rik)
NM 144541	Brain and reproductive organ-expressed protein (Bre)
NM 145711	Thymocyte selection-associated HMG box gene (Tox)
NM 172148	cDNA sequence BC028440 (BC028440)
NM 009342	t-Complex testis expressed 1 (Tctex1)
NM 009821	Runt related transcription factor 1 (Runx1)
NM 010149	Erythropoietin receptor (Rpor)
NM 011178	Proteinase 3 (Prtn3)
NM 013585	Proteosome (prosome, macrepain) subunit, beta type 9 (large multifunctional protease 2) (Psmb9)
NM 013814	UDP-*N*-acetyl-alpha-D-galactosamine:polypeptide *N*-acetylgalactosaminyltransferase 1 (Galnt1)
NM 013899	Translocase of inner mitochondrial membrane 13 homolog a (yeast) (Timm13a)
NM 018782	Calcitonin receptor-like (Calcrl)
NM 025570	Mitochondrial ribosomal protein L20 (Mrpl20)
NM 026479	DNA segment, Chr 11, ERATO Doi 416, expressed (D11Ertd416e)
NM 026965	Catechol-*O*-methyltransferase domain containing 1 (Comtd1)
NM 028906	Dipeptidylpeptidase 8 (Dpp8)
NM 030066	Armadillo repeat containing, X-linked 1 (Armcx1)
NM 133786	SMC4 structural maintenance of chromosomes 4-like 1 (yeast) (Smc4l1)
NM 148934	Gene trap ROSA b-geo 22 (Gtrgeo22)
NM 172562	Transcriptional adaptor 2 (ADA2 homolog, yeast)-like (Tada2l)
NM 173440	Nuclear receptor interacting protein 1 (Nrip1)
NM 177342	TAF5 RNA polymerase II, TATA box binding protein (TBP)-associated factor (TAF5)

encoding a membrane protein ($CD34^-KSL$: 122, SP Lin^-: 291, both populations: 118), we could use cell-function classifications to identify novel HSC cell surface marker candidates. These included cell adhesion, a biological process ($CD34^-KSL$: 10, SP Lin^-: 15, both populations: 7), and receptor activity, a molecular function ($CD34^-KSL$: 29, SP Lin^-: 72, both populations: 22). Indeed, among genes specific to $CD34^-KSL$ and/or SP

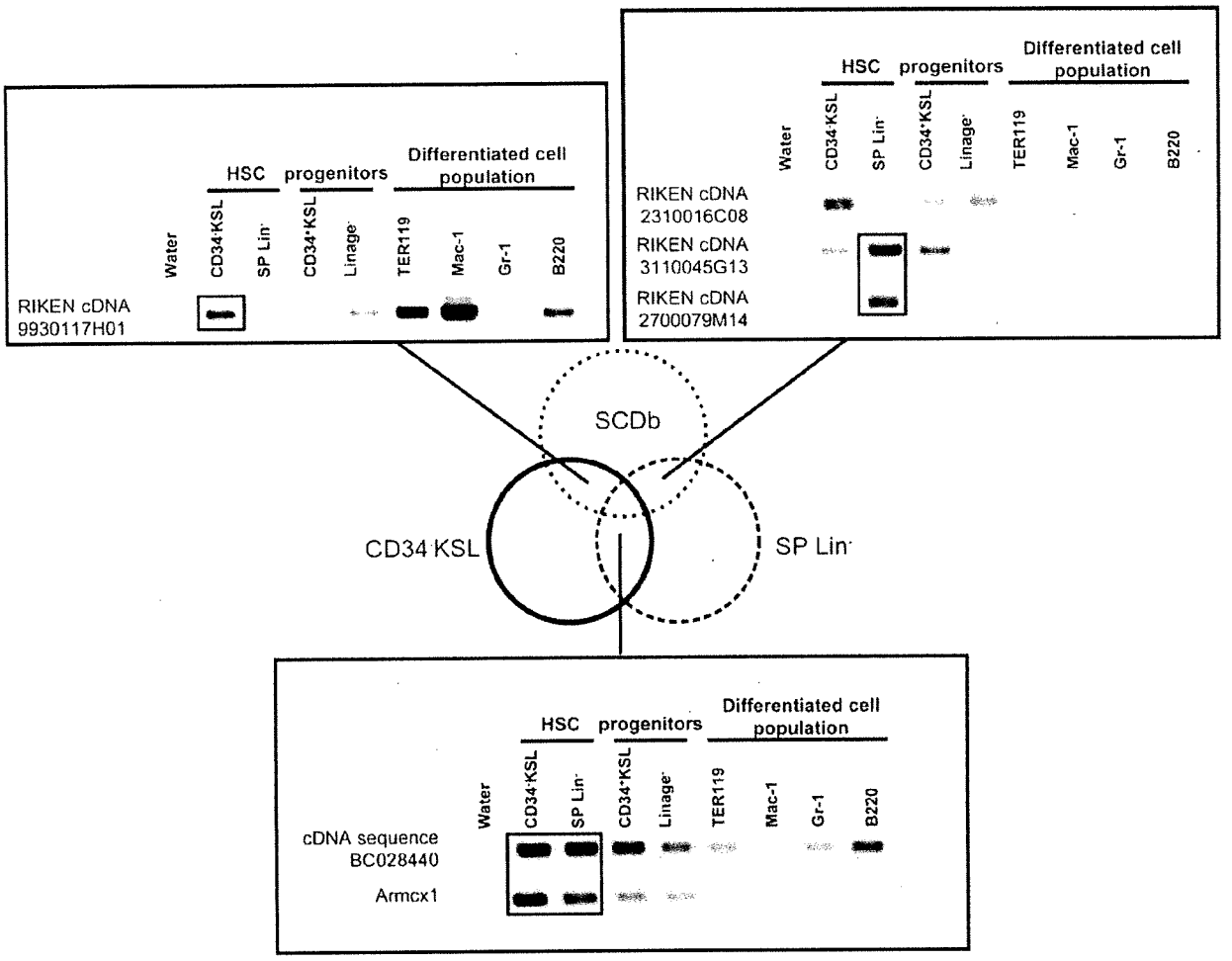

Fig. 5 Expression of identified genes. Expression of selected SCDb-listed genes shared between $CD34^-KSL$ cells and SP Lin^- cells and selected genes shared only between $CD34^-KSL$ cells and SP Lin^- cells was analyzed by RT-PCR. Cells analyzed are BM $CD34^-KSL$ and SP Lin^- HSCs, $CD34^+KSL$ and Lineage marker$^-$ progenitors, $TER119^+$ erythroblasts, Mac-1^+ monocytes/macrophages, Gr-1^+ neutrophils, and $B220^+$ B cells

Lin^- cells, the deduced amino acid sequence of RIKEN cDNA 9930117H01 contains both a putative signal peptide sequence and a transmembrane domain (Fig. 5). RIKEN cDNA 3110045G13 is similarly predicted to encode a cell surface transmembrane protein with extracellular EGF-like domains, and RIKEN cDNA 2700079M14 to encode a transmembrane protein with an extracellular immunoglobulin-like domain. To analyze expression specificities and functions of these putative cell surface proteins in HSCs would be intriguing. The GO profiling may help in understanding the molecular machineries operating in HSCs.

One of the most surprising results to emerge from mammalian cDNA sequencing projects is that thousands of mRNA-like non-coding RNAs are expressed, constituting at least 10% of poly(A)$^+$ RNAs [24, 25]. Non-coding RNAs are involved in the regulation of epigenetic functions, including chromatin structure and genome imprinting. Inactivation of the X chromosome by *Xist* RNA is a representative function of non-coding RNAs [26]. Some functions of non-coding RNAs in hematopoiesis have been reported [18, 19]. In most cases, however, the functions of these RNA molecules remain unclear. The biological significance of mRNA-like non-coding RNAs in HSCs in particular has not been clarified. We screened HSC clones for mRNA-like non-coding RNAs and identified 29 candidates. Our data suggest that some mRNA-like non-coding RNAs function in an HSC-specific manner. Understanding of the functions of HSC-specific mRNA-like non-coding RNAs would break open a new field of HSC biology.

By high-throughput sequencing analysis, we have added a number of genes to the list of HSC-specific genes and have identified HSC-specific putative mRNA-like non-